

Application Grade Thesis

Title: Development of an acoustic platform for the molecular diagnosis at the
point-of-care

Τίτλος: Ανάπτυξη μιας ακουστικής πλατφόρμας για τη μοριακή διάγνωση
στο σημείο παροχής φροντίδας

Student's Name: Angelos Ntimtsas

Supervisor's Name: Prof. Electra Gizeli

Date of completion: February 15, 2022

*This dissertation is submitted as a partial fulfilment of the requirements for the Master's degree of
Biomedical Engineering M.Sc. program*

Acknowledgements

First of all, I would like to thank my Supervising Professor Electra Gizeli, for the opportunity she gave me to work in her laboratory and take my first steps in the amazing world of biosensors. I would also like to thank her for assigning the subject of this work, and for the undivided help and knowledge she offered me during the realization of the experiments.

I am also thankful to Dr. Achilleas Tsortos for taking the time to introduce me to the acoustic concepts and providing me with valuable assistance and suggestions.

Next, I would like to acknowledge the people that I worked with in the lab, Dr. Dimitra Chronaki, Foteini Papagavriil, Anna Dimitriadi, Dr. Ilya Reviakine, Agapi-Eirini Simaiaki, Iro Beligianni, Sofia Spinthaki, Dr. Nikoletta Naoumi, Maria Megariti, Dr. Tassos Samarentsis, Katerina Hartle-Mougiou, Arianna Cimmarrusti, Dr. Martha Valiadi, Vaia Tsiakalou, Dr. Emilia Grypioti, Ioannis Svoliantopoulos, Stelios Grammatikos, Theologia Morfoniou and Myrsini Froudaki, for their continuous support, their suggestions and the collaborative environment.

Finally, I could not miss my parents and my sister, to whom I owe the biggest thanks for their love and support. Despite the difficulties they face, they did not stop for a moment to support me all these years.

Abstract

In the first part of the present dissertation, we present a brief review on the field of biosensors with special emphasis to recent applications related with emerging health related topics. Starting from a brief historical review about the development of the first biosensors, the basic characteristics and concepts of biosensors are discussed. Novel biosensing concepts and categories have been developed recently, therefore a brief state-of-art review to the main types and biomedical applications, is presented. Finally, we introducing key developments in the field of acoustic/piezoelectric biosensors, and illustrating the wide area of biomolecule detection capabilities, along with the numerous advantages that are present on this type of sensors.

In the second part of this study, it is presented the development of a low-cost and integrated surface acoustic wave (SAW) platform for the detection of molecular targets. The objective of this study is to establish a proof-of-concept application and addressing simultaneously several challenges related to technological and scientific topics. At the first step, we evaluated and explore the capabilities and the limitations of two widely used piezoelectric devices, specifically quartz and lithium tantalate. The latter presented extensive noise over the working frequency spectrum, while an attempt to minimize the spurious response was done. By testing the two different devices upon viscous loading with glycerol standards, quartz devices were found to be more sensitive over the different concentrations of glycerol concentrations. Concurrently with the evaluation of the acoustic devices, an attempt to use cost-effective, compact and open-source code instrumentation was done successfully.

The next step towards the development of the platform was the re-use of acoustic devices and introducing alternative microfluidic designs to reduce the overall cost. Quartz devices were tested over a great number of experiments and different surface cleaning approaches were evaluated, indicating that rinsing and gently scrubbing the devices with a cotton bud or swab can prolong the device's life up to 13 tests. Furthermore, experimental microfluidic gasket prototypes were made from common material and tested for their ability to maintain the acoustic signal and supplying the sensors surface with analytes without leaks.

Finally, the developed setup and protocol was tested for its ability to detect molecular targets. For this reason, the acoustic response was monitored over different concentrations of *Salmonella* DNA LAMP amplicons, indicating that in our approach the SAW platform has a limit-of-detection of 100 bacterial cells.

The results of the present study indicate that for the development of a portable acoustic platform several biological and engineering parameters should be optimized, thus, future research will focus mainly on alternative solutions to microfluidics, simplifying the instrumentation and increasing the sensitivity of the setup.

Περίληψη

Στο πρώτο μέρος της παρούσας διατριβής παρουσιάζεται συνοπτικά το πεδίο των βιοαισθητήρων δίνοντας έμφαση σε πρόσφατες εφαρμογές που αφορούν τον τομέα της υγείας. Αρχικά δίνεται μια σύντομη ιστορική αναδρομή σχετικά με την ανάπτυξη των πρώτων βιοαισθητήρων, και στη συνέχεια περιγράφονται οι βασικές κατηγορίες και τα χαρακτηριστικά τους. Παράλληλα, παρουσιάζεται μια σύντομη βιβλιογραφική ανασκόπηση για κάθε τύπο βιοαισθητήρα, εισάγοντας τις πιο πρόσφατες έννοιες, τεχνολογίες και βιοϊατρικές εφαρμογές. Τέλος, ιδιαίτερη έμφαση δίνεται στις βασικότερες εξελίξεις στον τομέα των ακουστικών/πιεζοηλεκτρικών βιοαισθητήρων, αναδεικνύοντας τα πολυάριθμα πλεονεκτήματά τους, και το ευρύ φάσμα εφαρμογών.

Στο δεύτερο μέρος της μελέτης, παρουσιάζεται η σχεδίαση και ανάπτυξη μιας φορητής και χαμηλού κόστους πλατφόρμας επιφανειακών ακουστικών κυμάτων (Surface Acoustic Wave, SAW) για την ανίχνευση μοριακών προϊόντων (DNA). Σε πρώτο βήμα, αξιολογούνται οι δυνατότητες και οι περιορισμοί δύο διαδεδομένων πιεζοηλεκτρικών υποστρωμάτων, συγκεκριμένα του χαλαζία (Quartz) και του τανταλικού λιθίου (LiTaO_3). Το τελευταίο υπόστρωμα παρουσίασε σε ολόκληρο το φάσμα συχνοτήτων εκτενή θόρυβο, και έγινε προσπάθεια ελαχιστοποίησης αυτού. Από τις μετρήσεις των ακουστικών αποκρίσεων σε πρότυπα γλυκερόλης με διαφορετικό ιξώδες, βρέθηκε πως οι αισθητήρες με υπόστρωμα χαλαζία είναι πιο ευαίσθητοι. Παράλληλα με την αξιολόγηση των ακουστικών υποστρωμάτων, παρουσιάζεται με επιτυχία η χρήση ενός αναλυτή ανοικτού κώδικα και εξοπλισμού χαμηλού κόστους.

Το επόμενο βήμα προς την ανάπτυξη της πλατφόρμας, είναι η αξιολόγηση της ικανότητας επαναχρησιμοποίησης των ακουστικών αισθητήρων και παράλληλα η μελέτη εναλλακτικών προσεγγίσεων στην κατασκευή κυψελών ελεγχόμενης ροής για τη μείωση του συνολικού κόστους. Συγκεκριμένα, οι αισθητήρες χαλαζία δοκιμάστηκαν για μεγάλο αριθμό πειραμάτων και αξιολογήθηκαν διαφορετικές προσεγγίσεις ως προς τον καθαρισμό της επιφάνειας, υποδεικνύοντας πως το ξέπλυμα με νερό και το απαλό τρίψιμο των συσκευών με βαμβάκι ή βαμβακοφόρο στειλέο μπορεί να παρατείνει τη διάρκεια ζωής του αισθητήρα έως και 13 δοκιμές. Επιπλέον, κατασκευάστηκαν πειραματικές διατάξεις μικροκυψελών ροής από κοινά εργαστηριακά υλικά και εξετάστηκαν ως προς τη διατήρηση του ακουστικού σήματος και στην τροφοδότηση της επιφάνειας των αισθητήρων με δείγματα, αποφεύγοντας τυχόν διαρροές.

Τέλος, η διάταξη και το πρωτόκολλο που παρουσιάζονται, δοκιμάστηκαν για την ικανότητά τους να ανιχνεύουν μοριακούς στόχους. Συγκεκριμένα, χρησιμοποιήθηκε DNA βακτηριακών κυττάρων *Salmonella*, που προέκυψε ύστερα από ισόθερμη αντίδραση πολλαπλασιασμού με τη χρήση της μεθόδου LAMP. Τα αποτελέσματα υποδεικνύουν πως η παρούσα ακουστική διάταξη δύναται να εντοπίσει έως και 100 βακτηριακά κύτταρα. Συμπερασματικά, τα ευρήματα της παρούσας μελέτης υποδεικνύουν πως για την ανάπτυξη μιας φορητής ακουστικής πλατφόρμας θα πρέπει να βελτιστοποιηθούν αρκετές βιολογικές και τεχνολογικές παράμετροι, επομένως, περαιτέρω έρευνα θα επικεντρωθεί κυρίως σε εναλλακτικές λύσεις στα συστήματα μικρο-ρευστομηχανικής (microfluidics), στην απλοποίηση της απαιτούμενης οργανολογίας και στην αύξηση της ευαισθησίας.

Table of contents

Contents

Acknowledgements.....	2
Abstract.....	3
Περίληψη.....	4
Table of contents	5
List of figures.....	6
Chapter 1: Introduction	8
Chapter 2: State-of-the-art	11
Chapter 3: Research methodology	21
Chapter 4: Results and discussion.....	26
Chapter 5: Conclusions	41
References	43
Appendices.....	55

List of figures

Fig. 1: (a) SENSEOR network analyzer with extension board (green PCB) capable to monitor in parallel the four different channels of the array; (b) NanoVNA network analyzer with two ports and embedded display. **Page 22**

Fig. 2: NanoVNASaver software that was modified for the needs of real-time amplitude and phase measurements (red and blue lines, respectively). **Page 23**

Fig. 3: (a) Polycarbonate docking station with microfluidic card and PCB heaters; (b) PCB prototype docking station. **Page 24**

Fig. 4: (a) Microfluidic card with two channels and the path of the liquid inside the channel (orange); (b) Lithium tantalate array at 155 MHz with interdigital transducers (IDTs) near the sensing area; (c) Quartz array at 155 MHz with dense network of IDTs. **Page 27**

Fig. 5: Images of acoustic signal spectra: (a) Lithium tantalate in air; (b) Quartz in air; (c) Lithium tantalate with water filling the microfluidic card; (d) Quartz with water filling the microfluidic card. **Page 28**

Fig. 6: (a) Lithium tantalate array with parafilm absorbers; (b) Lithium tantalate acoustic response with parafilm absorbers; (c) Lithium tantalate acoustic response with parafilm absorbers and water filling the microfluidic card. **Page 29**

Fig. 7: Real-time representation of the acoustic wave amplitude and phase using a lithium tantalate device. Series of injections was as follows: 1, 2.5, 5, 10, 20% (v/v) glycerol. The blue and black lines correspond to changes in phase and amplitude, respectively. Both phase and amplitude are measured in bits. **Page 30**

Fig. 8: Network analyzers comparison using a lithium tantalate device and glycerol calibration: (a) NanoVNA; (b) SENSEOR VNA. **Page 31**

Fig. 9: Real-time representation of the acoustic wave amplitude and phase using a quartz device. Series of injections was as follows: 1.25, 2.5, 5, 10, 15, 20, and 30% (v/v) glycerol. The blue and black lines correspond to changes in phase and amplitude, respectively. Both phase and amplitude are measured in bits. **Page 32**

Fig. 10: Glycerol calibration of quartz device by using SENSEOR network analyzer. **Page 33**

Fig. 11: Frequency drift of quartz devices over the number of experiments with two different cleaning methods: (a) air-plasma cleaning; (b) cotton bud cleaning. **Page 34**

Fig. 12: Real-time binding curves of LAMP reactions flowing sequentially over the four different sensing areas of the array. The blue and black lines correspond to changes in phase and amplitude, respectively. Both phase and amplitude are measured in bits. **Page 36**

Fig. 13: Amplitude attenuation obtained during the detection of dsDNA amplicons produced during LAMP of 100, 10^3 , 10^4 , 10^5 Salmonella cells (positive, green bars) and samples

containing no cells (negative, red bars) using an acoustic waveguide device functionalized with PLL(25)-g-PEG(2); (a) Δ Amplitude in bits; (b) Δ Amplitude in dB. **Page 38**

Fig. 14: Amplitude attenuation of each channel of the acoustic device (i.e., IDT) during the detection of dsDNA amplicons produced from LAMP reaction with 100 *Salmonella* cells (positive, green bars) and samples containing no cells (negative, red bars) using an acoustic waveguide device functionalized with PLL(25)-g[3.5]-PEG(2); (a) Δ Amplitude in bits; (b) Δ Amplitude in dB. **Page 38**

Fig. 15: Microfluidic gasket prototypes placed in a polycarbonate sheet with drilled inlets and outlets (metal pins): (a) thick parafilm gasket; (b) thin parafilm gasket; (c) double-sided tape; (d) brass docking station with parafilm gasket. The blue valve in the polycarbonate sheet was intended as bubble bleeder for future use. **Page 39**

Fig. 16: Docking station prototypes: (a) brass made base with adjustable pressure mechanism; (b) PCB docking station with neodymium magnets. In both cases, the SAW device was placed on a microscope slide patterned with parafilm window for the device. (c) Lithium tantalate response with the thick parafilm microfluidic gasket. **Page 40**

Chapter 1: Introduction

The advent of a new type of diagnostics that do not require specialized equipment, laboratory staff and facilities, make it possible for various diagnostic tests to find application near the patient, even in remote areas. Point-of-care (PoC) diagnostics target proteins, nucleic acids, metabolites and dissolved ions, drugs, cells, and microbes in samples that can be blood, saliva, urine, or other bodily fluids or (semi)solids (Gubala et al., 2011; Kumar et al., 2021). The current conventional diagnostic methods, such as identification of microorganisms by culturing samples or by performing enzyme linked immunosorbent assay (ELISA) and nucleic acid testing (NAT) using polymerase chain reaction (PCR), are usually performed in medical laboratories (Kumar et al., 2021). However, their applications are always limited due to their shared disadvantages such as time-consuming, labour-intensive, high cost, expensive machine dependent, and inability to achieve rapid on-site detection (Wang et al., 2021). To overcome these limitations, POC diagnostics introduce methods that provide the results rapidly, without requiring specialized instrumentation, therefore can be used at home or in the field.

Currently, two broad types of technologies have been established in the point of care (PoC) testing: small bench top analyzers (for example, blood gas and electrolyte systems) and hand-held, single use devices such as lateral flow tests that examine urine albumin, blood glucose, and cancer biomarkers) (Price, 2001; Sajid et al., 2015; Syedmoradi et al., 2021). Today, two important criteria in order for diagnostic platform to be viable in the developed-world market are the clinical usefulness and cost. These criteria are also applicable for global health, however the technical approaches to address them cannot always be transferred to low-resource settings (Yager et al., 2008; Balsam et al., 2013; Majors et al., 2017).

In recent years, many types of biosensors have been developed and used in a wide variety of analytical tasks, and mainly focus in the biomedical and environmental monitoring (Rasooly & Herold, 2009). A biosensor is based on two crucial parameters, a biological recognition element (ligand) that facilitates specific binding or biochemical reaction with the target analyte (e.g., antigen or DNA sequence) and a signal conversion device (transducer) (Prickril & Rasooly, 2017). Biosensors are categorized into four basic groups: optical, mass, electrochemical and thermal, depending on the method of signal transduction (Rocha-Gaso et al., 2009). An interesting field, which finds several biosensing applications (nucleic acids, proteins and metabolites) is the acoustic wave biosensors and they are categorized as mass sensors which operate with mechanical acoustic waves as their transduction mechanism (Rickert et al., 1999).

The surface acoustic wave (SAW) is an acoustic (i.e., mechanical) wave that propagates close to the surface of a specific-cut piezoelectric crystal (e.g., quartz, lithium tantalate, lithium niobate) (Shiokawa & Kondoh, 2004; Gronewold, 2007). The first report of a SAW transducer dates back to 1965, where a pair of interdigital transducers (IDT) was applied on the surface of a piezoelectric crystal, specifically ST cut quartz (White & Voltmer, 1965). Since then, SAW devices met extensive optimization of the aforementioned features and mainly found applications in electronics and telecommunications as compression/bandpass filters and resonators (Morgan, 1998). Until nowadays, SAW devices dominated the electronics market (total market above 2 billion units per year, 0.09\$ per SAW filter at 2008) (Aigner, 2008), however with the advent of the 5G era and high frequency demands, BAW (bulk acoustic wave) filters will dominate the market the upcoming years (by 2022, the global filter market size will exceed \$15 billion) (Peng et al., 2021; Yandrapalli et al., 2021). The first sensing application that implemented SAW devices as detectors was introduced by Wohltjen & Dessy (1979), where they performed an evaluation of quartz and lithium niobate along with the proper instrumentation to detect gaseous molecules and their pressure as a function of amplitude, phase and frequency. Latter publications presented the first biosensing applications of the SAW sensors, by detecting the binding of DNA molecules (Andle et al., 1991) and the absorption of human-IgG (Gizeli et al., 1992). The latter study, reported the enhancement of sensitivity upon application of a thin polymer layer, specifically polymethyl-methacrylate (PMMA), which acts as a resonating film and waveguides the produced waves on the surface of the device. The application of waveguide layers on the surface of SAW devices reduces the acoustic losses into the bulk that cause high noise levels, due to the diffraction and background interference from reflections of the acoustic signal. The guided shear-horizontal wave is called Love wave (Zhang et al., 2021).

Up to now there are several reports of SAW biosensing applications, however several limitations regarding the sensitivity, reproducibility and sustainability restrain the commercial availability of these setups to the biosensors market. As it is summarized by Länge et al. (2008), a market-compatible biosensor should be affordable, including the costs of production and implementation, durable for multiple uses and optimized in the context of electronic and microfluidic periphery.

The goal of the present study is to develop a fully automated POC platform that implements the loop-mediated isothermal amplification (LAMP), that amplifies DNA targets (i.e., genetic and infectious diseases) with high specificity, efficiency and rapidity under isothermal conditions (Notomi et al., 2000), and detects the amplified products by using the surface acoustic wave technology. To the best of our knowledge, up to now there are no reports of portable SAW platform that can operate in the field and utilizes low-cost microfluidic methods to introduce the samples on the sensor surface. So far, there is one commercially available option (i.e., Biosensor sam5 by SAW Instruments GmbH), which is dedicated for research. Previous reports that presented portable SAW approaches (Nguyen et al., 2017, Papadakis et al., 2018), use syringe pumps and microfluidic channels, constructed

by using specialized methods (i.e., plasma etching, spin coating) and facilities (i.e., clean rooms and machinery). In this work, an extensive study on the investigation of each aspect of developing an acoustic platform and alternative microfluidic channel prototypes is presented. Starting with the evaluation and the characterization of two available piezoelectric substrates (i.e., lithium tantalate and quartz) using glycerol standards, quartz was selected due to its high sensitivity, low in air losses and low noise threshold. Moreover, an investigation on reducing the cost and selecting the proper electronic instrumentation (i.e., vector network analyzers) was done, along with the modification of a commercially available and low-cost instrument. Due to the need for a user-friendly and re-usable platform, alternative cleaning methods were evaluated, suggesting that after each experiment, cleaning the surface of the sensor with a cotton bud is an effective solution and prolongs the life-span of the device. Furthermore, rapid microfluidic prototypes were made in order to avoid the use of micromachining methods, however technical limitations (i.e., leaks and attenuation of the acoustic signal) suggest that further optimization should be done in this direction. Finally, using an optimized acoustic detection protocol, a DNA amplified target of *Salmonella* cells was detected, suggesting better discrimination between the control and positive samples and reaching a limit of detection of 100 copies. The results so far suggest the important factors and features that potentially can reduce the manufacturing cost and increase the efficiency of such a platform and therefore develop a versatile tool for the detection of multiple molecular targets.

Chapter 2: State-of-the-art

History of biosensors

During the last two centuries human civilization made huge steps in multiple fields, especially in biology and engineering. The rapid development of methods, applications, models and tools made it possible for the modern world to personalize each innovation or application to the needs of the individuals. From simple household devices up to complex instruments that are used in medical or industrial settings, sensors are a key element for a machine to interact with its environment and provide sufficient information to a process unit or an actuator, in order to take the proper decision or action. Among different fields, the concept of a sensor may be slightly different and it should be adjusted to the needs of the application, however the requirements remain somehow the same. A sensor unit should be able to provide accurate and precise measurements of the environment, and ideally should be affordable and miniaturized (Mandal & Banerjee, 2022).

One of the most prominent fields of developing specialized sensors is that of biomedical devices. The first report that introduced the concept of an early form of such a sensor date back to 1906, when M. Cremer showed that the electrical potential of a liquid that is separated by a glass membrane is proportional to the concentration of the acid that is diluted in the liquid (Cremer, 1906). Few years after the observation that was made by Cremer and the introduction of the concept of hydrogen ion concentration in fluids, the well-known pH (Sørensen, 1909), W.S. Hughes discovered in 1922 a novel electrode that was made from an empty glass bulb and it was able to determine the pH of a liquid by measuring the voltage difference between the electrolytes on each side of the glass bulb (Hughes, 1922). Until 1956, the sensors that were developed were limited to the analysis of liquids and enzymes (Bhalla et al., 2016), however Leland C. Clark, also known as the “Father of Biosensors”, was about to change the entire field of biosensing applications. As it is described in the biography of Leland C. Clark (Heineman & Jensen, 2006), during the development of a heart-lung support device for surgeries, Clark introduced two novel devices. His first invention inspired from the need to monitor oxygen levels in the blood of the patient during the surgery and that was done visually by a specialist. Clark, experimented with an oxygen sensor, however, upon contact of the sensor with blood, the signal was saturated due to blood coagulation. Interestingly, he tackled the problem by covering the sensor with a cellophane membrane from a pack of cigarettes which protected the sensor’s surface while it was permeable to oxygen (Heineman & Jensen, 2006). Later in 1962, while he was calibrating the oxygen sensor by using an enzyme that converts glucose and oxygen to hydrogen peroxide, he realized that such a reaction eventually can be incorporated into a system and develop a blood-glucose sensor (Clark & Lyons, 1962; Heineman & Jensen, 2006).

Even though the field of biosensors started to develop from the very beginning of the previous century, it is unclear which was the starting point that biosensors were established as a sub-field of biomedical research and diagnosis (Olson & Bae, 2019). By searching the term “biosensor” on the database of PubMed, up to now, there are 83,233 publications starting from the year 1965 and include several results that are associated with the development of sensors for various applications, such as environmental monitoring. However, there are only 15,174 publications from 1981 that are dedicated to the medical field and most of them published during the last 12 years.

The concept of biosensors

A biosensor is a device or probe that integrates a biological recognition element, such as an enzyme or antibody, and with the use of an electronic component or a reaction, a measurable signal is generated/obtained (Naresh & Lee, 2021). As it is summarized by Bhalla et al. (2016), a typical biosensor comprises from five different components, an analyte, a bioreceptor, a transducer, the electronic circuitry and a display. Starting from the first component, an analyte is the molecule or substance of interest and it can be a protein (such as an enzyme or an antibody), a DNA molecule, or even chemical entity (i.e., toxins or heavy metals) (Odobasić et al., 2019). In order for the analyte to interact with the biosensor a recognition element it is required. That component can be an antibody, enzyme, microorganism, organelle, cell receptor or even a DNA probe molecule (Tetyana et al., 2021). Based on the type of sensing molecule that is used for the detection of the analyte, biosensors can be divided into enzyme-based, DNA-based sensors, immunosensors, and so on (Yoon et al., 2020). Upon binding of the target molecule on the biorecognition element, a signal is generated with the form of light, heat, change in pH, change of the electric potential or change of mass (Bhalla et al., 2016). For example, the interaction of an analyte such as the human chorionic gonadotropin (hCG), a key pregnancy hormone that is present in circulation and urine, can be detected through the affinity for the hCG antibodies that are used at point-of-care tests (Cole, 2012). The main element of all biosensors is the transducer, which is responsible for converting the aforementioned signals or changes into other forms of energy, for example voltage potential (Tetyana et al., 2021). Most biosensing applications include also the required electronic periphery to amplify and/or filter the signal that is obtained from the transducer, and convert it into a digital form that can be later represented into a display (Bhalla et al., 2016). However, the latter two components are not essential for all the different types of biosensors that are used in the medical field. A great example of a simplified device which is well-established all around the world due to the low-cost and its simplicity, while it does not require electronic periphery is the lateral-flow immunoassay for SARS-CoV-2, where the signal is obtained via a color change or the appearance of a line in a nitrocellulose membrane (Di Nardo et al., 2021). Based on the transduction methods that are utilized, biosensors can be categorized into five different main classes: electrochemical, electrical, optical, piezoelectric (mass detection methods) and thermal detection (Monošík et al., 2012).

Characteristics of biosensors

Even though there are different categories and sub-classes that cover the field of biosensors, regardless the type that is used, due to the demanding nature of detecting analytes in the molecular level, some important criteria should be met in order a sensing device to be useful and effective for each application. As it summarized by several review articles (Bhalla et al., 2016; Malhotra et al., 2018; Tetyana et al., 2021; Naresh & Lee, 2021) biosensors should be selective, sensitive, stable, present linearity, provide reproducible measurements in a short amount of time and most importantly to provide the lowest possible detection limit. Regarding the sensitivity of the biosensors, which is considered as the most important and vital parameter for precise detection/diagnosis (Haleem et al., 2021), is defined as the magnitude of sensor's response with respect to the concentration of the target molecule that is presented on the sample (Malhotra & Ali, 2018). A sensitivity associated parameter is the limit of detection (LOD) of a sensor, which describes the ability of a sensor to detect the lowest possible concentration of the target molecule and can be used to define the quality of a system to detect analytes and compare it to similar setups (Karunakaran et al., 2015; De Vicente et al., 2020). However, the increased sensitivity of a biosensor is not by itself an adequate parameter that can characterize a device suitable for an application.

Biosensors over the years have been applied in several fields like the food industry and quality control of the products, in environmental monitoring settings and most importantly in the medical field for detecting diseases and infections (Mehrotra, 2016; Haleem et al., 2021). The samples that are analyzed with the use of biosensors on the aforementioned fields, are complex and multiple molecules are present. For example, in blood there are several proteins and cells that may have affinity for the bioreceptor that is located in the surface of the transducer, and the non-specific binding of the interfering molecules will result to erroneous results (i.e., false positive) (Karunakaran et al., 2015; Peveler et al., 2016; Rusling & Forster, 2021). Therefore, the selectivity of a biosensor is also an important attribute that should be considered during the design and functionalization of the transducer with a biological receptor (Polatoğlu et al., 2020; Tetyana et al., 2021).

Electrochemical biosensors

Starting with the electrochemical biosensors, compared to other types, this category is particularly useful for a number of applications due to their remarkable detectability, experimental simplicity and low cost, while they are also considered as label-free, meaning that it is not required labelling of the target molecule (e.g., with a fluorescent dye) (Stradiotto et al., 2003; Malhotra and Ali, 2018). In this category of biosensors an electrochemical reaction takes place on the surface of the transducer and therefore the analyte is detected by the produced electrochemical signal (Malhotra and Ali, 2018). The electrical potential difference that is generated by the interaction of the analyte and the ligand, is proportional to the concentration of the target molecule, therefore apart from qualitative results, quantification of molecules in a sample can be done (Tetyana et al., 2021).

Based on the signal that is generated, electrochemical biosensors can be further divided into amperometric (measure current change), potentiometric (measured pH and ions), conductometric (measure electric conductivity) and impedimetric/capacitive (measure changes in inductance and capacitance of samples) (Wang et al., 2008; Bahadır & Sezgintürk, 2016; Malhotra et al., 2018; Ding & Qin, 2020). A recent and highly promising application of an electrochemical biosensor for the detection SARS-CoV-2 was suggested by Ang et al. (2022), where the authors proposed the use of graphene oxide nanocolloids as an electroactive material that acted both as a transducer and as an electroactive label of the virus genomic sequences. The proposed method was based on the immobilization of a probe DNA sequence onto the surface of nanocolloids and upon the presence of the target analyte (2019-nCoV), the formation of the probe-target complex was achieved, allowing a direct correlation between the electrochemical signal arising from the target-colloids complex concentration over a wide linear range (i.e., from 1000pM to 0.1mM). At this point it should be noted that electrochemical enzyme-based biosensors are one of the most advanced and commercially successful bioanalytical devices because of the high sensitivity and selectivity of the enzymes that are used for the detection of targets (Kucherenko et al., 2019). A great example of commercially available products, are the enzyme-based glucose sensors, which are used by millions of people around the world (based on WHO, more than 420 million people are living with diabetes worldwide). Due to the large number of diabetic patients and the need for rapid, accurate and low-cost monitoring, many approaches for glucose electrochemical analysis have been developed the recent years and they have been incorporated into commercialized and research-level devices, from simple test strips, to wearable devices and implantable systems (Lee et al., 2018).

Optical biosensors

Another type of real-time analyte detection is the use of optical biosensors. A typical scheme is the measure of an optical signal which is sensitive to the change of refractive index in the proximity of the recognition element due to the binding of the target molecule (Zanchetta et al., 2017). They consist by four main components, a light source to generate the electromagnetic radiation, a combination of optical components to focus and propagate the light beam, a properly modified transducing surface, and a photodetector which records changes in the absorption, transmission, reflection, refraction, phase, amplitude, frequency and light polarization, in response to physical or chemical modifications that created by the interaction of biomolecules on the surface of the transducer (Naresh & Lee, 2021; Tetyana et al., 2021). The biorecognition molecules that can be immobilized in the transducer elements of optical biosensors are antibodies, enzymes, oligonucleotides, aptamers, hormone receptors, live cells and tissue (Damborský et al., 2016; Chen & Wang, 2020). As it presented by Fan et al. (2008) the optical sensor is surrounded by a chamber which is filled with a buffer solution. With the presence of target analytes, the affinity for the biorecognition molecules will result to the displacement of buffer molecules from the surface of the transducer, and that will cause the change of the refractive index, which will be recorded by the

instrumentation. The aforementioned methodology for monitoring the presence and the interaction of biomolecules, offers high sensitivity and stability, immunity to external disturbance and low noise (Chen & Wang, 2020). According to the detection method, optical biosensors can be designed as label-free or label-based. In label-free class the measured signal is produced directly by the interaction between transducer and the bio-analyte. On the contrary, in label-based sensing, the optical signal is generated by calorimetric, fluorescence, or luminescent (Fan et al., 2008; Damborský et al., 2016; Naresh et al., 2021). By comparing the two approaches, the label-free optical biosensors are a preferable solution since they require less expertise and effort to prepare an experiment, thus reducing the possibility of erroneous results, and they are also more economically efficient since they eliminate the need of specialized labelling molecules (Fan et al., 2008; Tabbakh et al., 2021). Due to the extensive research on optical biosensors, various transduction methods have been introduced over the years and they are based on the following optical phenomena: absorption, reflection, refraction, transmission, fluorescence/chemiluminescence, Raman scattering and surface plasmon resonance (SPR) (Malhotra et al., 2018).

From the aforementioned approaches, SPR biosensing appears to be one of the most powerful tools in the field of biomedical research for monitoring the affinity of biomolecules and study a variety of biological entities, such as DNAs, RNAs, proteins, carbohydrates, lipids, and cells (Nguyen et al., 2015). Briefly, the generation of surface plasmon resonance occurs when a focused light beam interacts with free electrons at a metal-dielectric interface (typically is gold) (Pitarke et al., 2007). Under certain conditions and specific beam angle, the influence of light energy will cause the electrons of the metal film to excite (i.e., surface plasmons) and start to propagate as an electromagnetic surface wave that is strongly localized across the metal interface (Abdulhalim et al., 2008; Nguyen et al., 2015). The generation of surface plasmons will result to the reduction of reflected light intensity at a specific angle, which is called resonance angle, and it is highly sensitive to changes near the metal surface (Abdulhalim et al., 2008; Damborský et al., 2016). Therefore, by measuring the shift of reflectivity, angle or wavelengths over time, quantitative and real-time changes of the refractive index can be recorded (Damborský et al., 2016).

Traditional SPR devices generally require expensive and bulky equipment, sophisticated optics, and precise alignment of the components, thus, increasing the number of difficulties for developing commercial and portable platforms in a low-cost for the point of care (PoC) (Prabowo et al., 2018; Moran et al., 2018; Tetyana et al., 2021). However, a novel approach for portable and rapid detection of SARS-CoV-2 virus, was developed by Huang et al. (2021). The researchers utilized specially designed periodic nanostructures that eliminate the need of complex optical apparatus. By developing a portable, low-cost, and smartphone-controlled reader, the samples can be loaded into a nanoplasmonic sensor chip cartridge, enabling real-time virus binding on the sensors surface. Interestingly, the device is able to detect virus particles in the range 0 to 6.0×10^6 vp/mL within 15 minutes, and it reaches the quantification limit of 4000 virus particles. The aforementioned approach is a great example of how optical biosensors can be designed to be affordable and accessible even in remote areas, finding applications near the patient as additional and alternate testing methods that

can generate results faster than the tests currently being used for COVID-19 testing (Sharma et al., 2021).

Piezoelectric biosensors

Another type of devices that can be used in biomedical applications enabling real-time, low-cost and label-free detection of analytes in liquid and gaseous media, is the acoustic wave (or piezoelectric) sensors (Länge, 2019). This category of biosensors is based on the piezoelectricity phenomenon and describes the ability of a material to generate an internal electric field when subjected to mechanical stress or strain (Berlincourt, 1971). The piezoelectric effect was discovered by the French physicists Pierre and Jacques Curie in 1880 as a way to monitor the charges that emitted by radium; however, it took about thirty years to find applications related to the generation of acoustic waves (Mason, 1981). The first report of using the piezoelectric effect for sensing applications it was made by Sauerbrey et al. (1959), proposing that the resonant frequency of a quartz crystal microbalance can be used for quantitative measurements of changes at the crystal surface. Since then, the acoustic wave technology was widely developed for various applications associated mainly with the industry. For example, they are used as telecommunication filters in mobile phones or as sensors for monitoring high temperatures in various manufacturing processes. They are also use to measure the stress/strain of materials automotive industry, in the biomedical sector as biosensors, even in military applications for use as radiofrequency filters in radars (Morgan, 1998, Drafts, 2001; Ruppel, 2017).

Piezoelectric materials can be organic (e.g., keratin, collagen, various polymers etc.), inorganic (e.g., quartz, lithium tantalate), even biomolecules (e.g., nucleic acid) that can convert mechanical force into electricity and vice versa (Pohanka, 2017; Chorsi et al., 2018). However, inorganic materials, like quartz, lithium tantalate, lithium niobate, aluminum nitride, zinc oxide, are the first choice for the fabrication of acoustic waves sensors due to well established processing methods that are required for the fabrication of these devices, such as photolithography and spin coating (Ramadan et al., 2017; Länge, 2019).

Independently of the different variations, the acoustic wave sensors are based on the property of inorganic piezoelectric materials to induce and propagate mechanical waves when an electrical oscillation of specific frequency is applied to them. Concurrently, they are able to convert the acoustic waves back into an electrical signal, which is strongly influenced by changes that happen in the resonance frequency, due to mass changes/perturbations that are generated in the sensing environment (Karunakaran et al., 2015; Fogel et al., 2016; Grammoustianou & Gizeli, 2018). Based on the way that the acoustic wave is propagated in the material, piezoelectric sensors are divided into two main categories, the bulk acoustic wave (BAW) devices, and the surface acoustic wave (SAW) devices (Fogel et al., 2016; Mehrotra, 2016). Regardless of the device that is used, the binding of analytes is normally followed by monitoring the velocity and/or energy change of the acoustic wave in real time. Measurements related to the former are normally recorded as frequency or phase change, while dissipation or amplitude attenuation is the reported signal related to the acoustic wave

energy (Grammoustianou & Gizeli, 2018).

The quartz crystal microbalance (QCM) is a BAW sensor and usually AT-cut quartz crystals are selected for the fabrication of the QCM devices due to the negligible temperature coefficient of this type, and therefore, better stability at room temperatures (i.e., 1 ppm/°C change of frequency in the range 10-50°C) (Alassi et al., 2017). A pair of electrodes are placed on the surface of the quartz crystal and by applying them an electrical oscillation the crystal plate will vibrate. The oscillation mode of QCM is called thickness-shear mode, which has the direction of displacement perpendicular to the quartz thickness and it is sensitive to mass and viscous changes that influence the frequency and the dissipation (QCM-D) of the oscillation, respectively (Na Songkhla & Nakamoto, 2021).

QCMs are a well-established approach for biosensing, however, there is a significant constraint regarding increasing the operating frequency in order to reach higher mass sensitivity. Even though it is possible to fabricate higher frequency QCM sensors, one should compromise with the fact that the devices will become thinner, thus, fragile and more difficult to handle (Länge, 2019). An interesting approach to tackle the aforementioned problem is the use of higher order harmonics. These higher odd number harmonic measurements have the advantage that the cheap, relatively thick, and easily-mountable low frequency crystals can be used at higher operating frequencies to increase mass sensitivity, for example a 10 MHz device can be monitored at the 11th harmonic (i.e., 110 MHz) (Kasper et al., 2016). However, monitoring the response of QCM devices at higher harmonic frequencies, require the use of more sophisticated and complex instrumentation (Na Songkhla & Nakamoto, 2021), thus it is difficult to transfer such a sensing technology to the point-of-care at low-cost.

A higher fundamental frequency alternative that was developed in parallel with QCM, is the SAW sensor, enabling the monitoring of analytes binding in gaseous and aqueous environments. SAW systems can operate in the frequency range of 100 MHz up to several GHz, providing higher mass resolution than QCM-based system, since the produced acoustic waves propagate in the surface of the piezoelectric substrate, where the interaction of molecules takes place (Fogel et al., 2016; Primiceri et al., 2018). Indicatively, in a recent publication by Lama et al. (2021), the comparison between a SAW and a QCM sensor revealed that a 250 MHz SAW device had 100 times greater sensitivity for detecting dimethyl methylphosphonate (DMMP) (a simulant for chemical warfare agents).

In comparison with the previously presented biosensor setups, SAW devices have numerous advantages in terms of detection capabilities in biomedical settings, since they are reliable, sensitive, selective, label-free and real-time, and can be produced at low-cost since several electronics manufacturers fabricated them for use in mobile phones (Banu Priya et al., 2014; Banu Priya et al., 2015; Balysheva, 2019). In addition to the well-established sensing applications that SAW devices can be used, this technology enables also various actuation applications in the microfluidics level. As it reviewed by Lei & Hu (2020), with proper design and by applying high power short pulsed, SAW devices can be used for manipulating fluids by creating jets and streams at the micro-nano scale. Similar applications using SAW devices as actuators have been developed the recent years with very promising results for the biological research and medical diagnosis. For example, they have been used for the label-free separation of circulating tumor cells (Ding et al., 2014), for assisting the proliferation and

dynamics of cell cultures by inducing the proper conditions (Greco et al., 2018), even making flexible platforms for performing various protocols on a chip with controlled injection and mixing of reagents (Zhang et al., 2018).

For the fabrication of surface acoustic wave devices, specific piezoelectric materials are selected. Depending on the application, the working frequency of the devices and the sensing environment (i.e., liquid or gas), a plethora of piezoelectric substrates have been used. The most commonly used piezoelectric materials for the fabrication of SAW devices are quartz, lithium niobate, lithium tantalate, langasite and lead zirconate titanate. Apart from the aforementioned inorganic bulk substrates, piezoelectric thin films like ZnO, AlN, PZT, PVDF, SiC, and polymer substrates, have been used for the fabrication of SAW devices (Nair et al., 2021; Mandal & Banerjee, 2022). At this point it is important to mention, that prior to the selection of a substrate, two important parameters should be considered. Specifically, the efficiency of the electromechanical conversion in a material, which is measured by its electromechanical coupling coefficient (K^2), and the zero-temperature coefficient of frequency (TCF). Materials with low electromechanical coupling coefficient will present high input losses, limited conversion of electric-acoustic energy, and in liquid biosensing applications the presence of aqueous solutions (e.g., water) will result to large attenuation of the surface acoustic waves (Länge et al., 2008; Devkota et al., 2017). Furthermore, materials with low coefficient of thermal expansion should be preferred in order to avoid temperature dependent frequency variations (Devkota et al., 2017; Mandal & Banerjee, 2022). This coefficient parameter can be modulated by changing the crystal cut, for example AT-, FC-, IT-, SC-, ST-cuts, and great research/modelling is done towards finding temperature insensitive cuts (Wang et al., 2018).

The next step upon the selection of the proper piezoelectric substrate is the fabrication of patterned metal electrodes on the surface, using conventional lithography techniques (Zakaria et al., 2014). These electrodes are called interdigital transducers (IDTs), they are usually made from aluminum, gold, or copper, and they transform the applied electrical energy from the instrument's oscillator (i.e., input IDTs) into mechanical energy which propagates in crystal's surface in the form of acoustic waves (Pannerselvam et al., 2018; Mandal & Banerjee, 2022). Bilaterally of the input IDTs, a second array of electrodes (i.e., output IDTs) is responsible for converting the mechanical energy of the propagated waves back to electrical oscillations. In the case of shear horizontal (SH) SAW sensors, a delay line made usually from aluminum or gold, is patterned in a significant distance between the input and output IDTs. The surface of the delay line is covered with a biological layer (e.g., antibody, DNA, or polymer), which has the proper affinity for the target molecule (Voiculescu & Nordin, 2012; Papadakis et al., 2017a). The absorption of the analyte on the sensitive layer will produce a shift in phase velocity (measured in degrees) due to mass deposition, and/or attenuation of the waves (i.e., amplitude, measured in decibels(dBs)) due to viscous changes on the sensor's surface (Voinova, 2009).

The anisotropic nature of the piezoelectric crystals that are used for the fabrication of SH-SAW sensors, results to several problems such as lateral diffraction of the waves over long regions, and in beam steering due to unmatched wave velocities along the X and Y axis, resulting to reduced wave propagation and ultimately to decreased sensitivity (Mei & Friend, 2019). In order to overcome these limitations, a thin layer of dielectric material is applied on the surface, which guides the propagating waves within the thickness of the film, thus the acoustic energy is strongly confined in the waveguide layer making the sensor more sensitive to mass changes (Mandal & Banerjee, 2022). These SAW devices are called Love wave sensors and different dielectric materials are used for coatings, such as polymers (e.g., SU8, parylene-C, PMMA, PDMS, PEI, PVA, carbowax etc.) and metal oxides (e.g., SiO₂, ZnO, TiO₂, SnO₂ etc.) (Pannerselvam et al., 2018; Caliendo & Hamidullah, 2019; Mandal & Banerjee, 2022). For the application of polymers simple and low-cost approaches can be used, like spin coating, solvent casting, dip coating and spray coating; however, the major drawback of this approach is the reduced polymer stability and reproducibility over time, while for metal oxides more demanding and expensive methods are required (e.g., ion beam assisted reactive deposition, chemical vapor deposition, RF sputtering etc.) (Pannerselvam et al., 2018). Regardless of the selected waveguide material, the applied layer should have lower acoustic shear velocity than that of the substrate (Gizeli et al., 2003), low density, excellent elastic and homogeneous properties, and most importantly low acoustic absorption (Laude, 2021; Tian et al., 2021).

A wide range of biosensing applications have been reported lately in the literature with promising results to transfer SAW technology at the point-of-care. A great advantage of SAW devices, is that based on the application, different surface functionalization approaches can be selected, making the sensor a versatile tool for monitoring different molecules in multiple environments. In a recent publication, Kus and co-workers (2021) developed a SAW device functionalized with gold nanorod (AuNR) and silver nanocube (AgNC) molecules to detect volatile organic compounds (e.g., toluene) that are present in exhaled breath of lung cancer patients. Apart from gas sensing applications, SAW sensors have been also used for the detection of proteins and DNA molecules. Specifically, Peng et al. (2021) demonstrated a no-wash, rapid, and quantitative immunoassay SH-SAW biosensor for the detection of SARS-CoV-2 antibodies. Interestingly, in their approach serum samples can be placed directly on the functionalized with virus nucleocapsid (N) protein surface, thus eliminating the need of pumps, tubing and microfluidic flow cells. Finally, a rapid handheld diagnostic device that utilizes SAW technology to detect DNA molecules, was developed by Branch et al. (2020). In their approach, a microfluidic disc was developed for SARS-CoV-2 RNA extraction/purification from nasal swab samples. Using quantitative reverse transcription PCR (RT-qPCR), the produced SARS-CoV-2 virus DNA amplicons were further amplified with the loop-mediated isothermal amplification (LAMP) reaction. Finally, the LAMP assay products could be detected in real-time using a SAW sensor embedded within a 3D-printed microfluidic flow cell.

Over the years, commercial SAW devices have been largely employed in everyday appliances, telecommunication products, and in automotive industry, while in the biomedical field, the applications of SAW sensors mostly remain in research settings. So far, several biosensing technologies have been described, however most SAW setups remain non-commercializable due to significant challenges associated with fabrication process, the integration of low-cost microfluidics and the damping effect of liquids in the acoustic signal (Zida et al., 2021). Furthermore, most of SAW sensing publications focus on the optimization of the waveguide materials, piezoelectric substrates, IDT and microfluidic arrangements, while an also important limitation for commercially available and portable setups, is the development of simplified, cost-effective, and user-friendly instrumentation (Nguyen et al., 2017; Depold et al., 2021).

Considerations

To conclude, the need for continuous health monitoring and diagnosis near the patient it is now more than ever evident. The field of biosensors, regardless the technology in use, require innovative and radical solutions to address the increasing healthcare needs around the world. There are several limitations to overcome in order to develop a cost-effective, compact, user-friendly and trustworthy setup for diagnosis and prognosis that can be also be useful in remote settings, where additional difficulties may apply. The increased sensitivity, label-free and real-time monitoring are some of the most important advantages that acoustic devices can offer in the medical sector, enabling either the installation of small benchtop setups for the analysis of patients' samples in healthcare units, either the development of portable devices for resource-poor settings. Even though the commercialization of SAW biosensors has not fully developed yet, the promising detection capabilities and the diverse area of sensing applications, in parallel with the mass production of low-cost commercial acoustic devices, may permit the development of a low-cost PoC-SAW platform in the near future.

Chapter 3: Research methodology

3.1. Reagents

The glycerol that was used for the titration experiments was purchased from Applichem GmbH (Darmstadt, Germany). PBS (pH = 7.4) and Tris (Trizma hydrochloride solution, pH = 7.5) buffer solutions were from Sigma-Aldrich (St. Louis, MO, USA). PLL(25)-g[3.5]-PEG(2) was purchased from Nanocs Inc (New York, USA).

3.2. Fabrication of SAW array

A SAW array (16 ×16 mm) comprising a 4-acoustic channel design was fabricated on two different substrates. The first type of device was fabricated on a ST quartz (YXl/36°) where each sensor included patterned 150 nm thick aluminum electrodes on top of a thin chromium layer, followed by a split-finger geometry resulting in 8 μm electrode period and 32 μm acoustic wave length. The operating frequency of quartz devices was 155 MHz. A waveguiding layer (1.2 μm thick) was formed with S1813 positive photoresist (Shipley, U.S.) using a spin coater (Specialty Coating Systems, INC, Spincoater P6700 series) at 850 rpm and for 30 s (Papadakis et al., 2017a). The application of the waveguiding layer over the entire array resulted in a decrease of the operating frequency at approximately 152 MHz. The final step for the preparation of the devices was the exposure of a specific area with UV light in order to remove the waveguide layer over the connection pads. Typical insertion losses of the quartz devices in air were between 18 and 27 dB.

The second type of device was fabricated on a lithium tantalate substrate (LiTaO₃, Y/36°), where each sensor included patterned 150 nm thick aluminum electrodes on top of a thin chromium layer, followed by a double-electrode design with periodically alternating length to eliminate the in-band mechanical reflections (Bristol et al., 1972; Malocha, 2004), resulting in a 6.6 μm electrode period and a 26.4 μm acoustic wave length. The operating frequency of the LiTaO₃ devices was 155 MHz and after the application of the waveguide layer (same procedure as to that of the quartz devices), the operating frequency dropped to approximately 152MHz. Typical insertion losses of the LiTaO₃ devices in air were in 20 dB range.

3.3. Analytical instrumentation

For the real time detection of amplitude and phase changes, two different vector network analyzers (VNA) were used. The first analyzer was developed by SENSEOR (Rabus et al., 2012, 2013) (Fig.1a) and is capable to sweep from 50 MHz up to 160 MHz using 400 data points. The analyzer consists from a programable RF oscillator and a RF detector, while by implementing 8 different high frequency switches, the analyzer monitors the four different channels of the SAW array sequentially. The recorded data are represented in bit units, while the conversion of the variation of amplitude from bits to dBs, can be done by multiplying the

ΔA values in bits with 0.0012926 (this factor was determined experimentally).

The second analyzer that was used is the NanoVNA-H (Fig. 1b), a standalone portable device with battery, capable to sweep from 50 KHz up to 900 MHz using 101 data points. The device is able to connect with a personal computer through a dedicated software (NanoVNASaver v0.3.9) (Fig. 2) and provide the various acoustic parameters every second. The software was modified properly in the Python Integrated Development Environment (PyCharm community edition 2021.2) in order to plot and record the amplitude and phase values over time. The connections between the analyzers and the devices were done by using coaxial cables terminated with SMA and IPEX RF connectors.

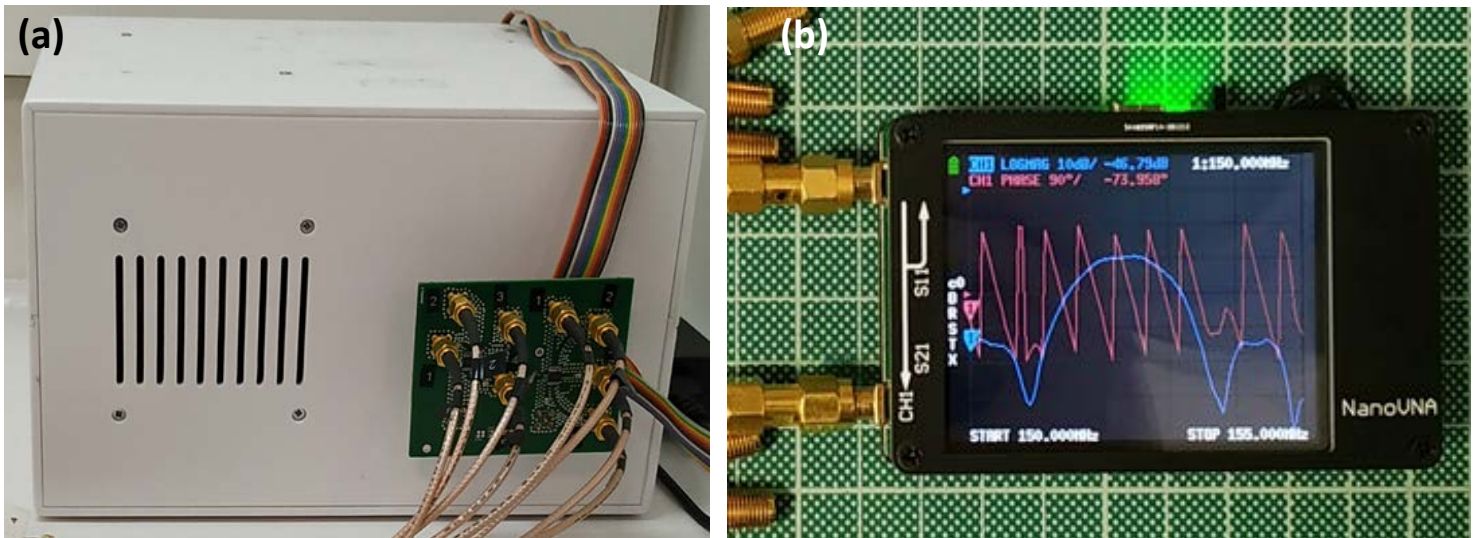


Fig. 1: (a) SENSEOR network analyzer with extension board (green PCB) capable to monitor in parallel the four different channels of the array; (b) NanoVNA network analyzer with two ports and embedded display

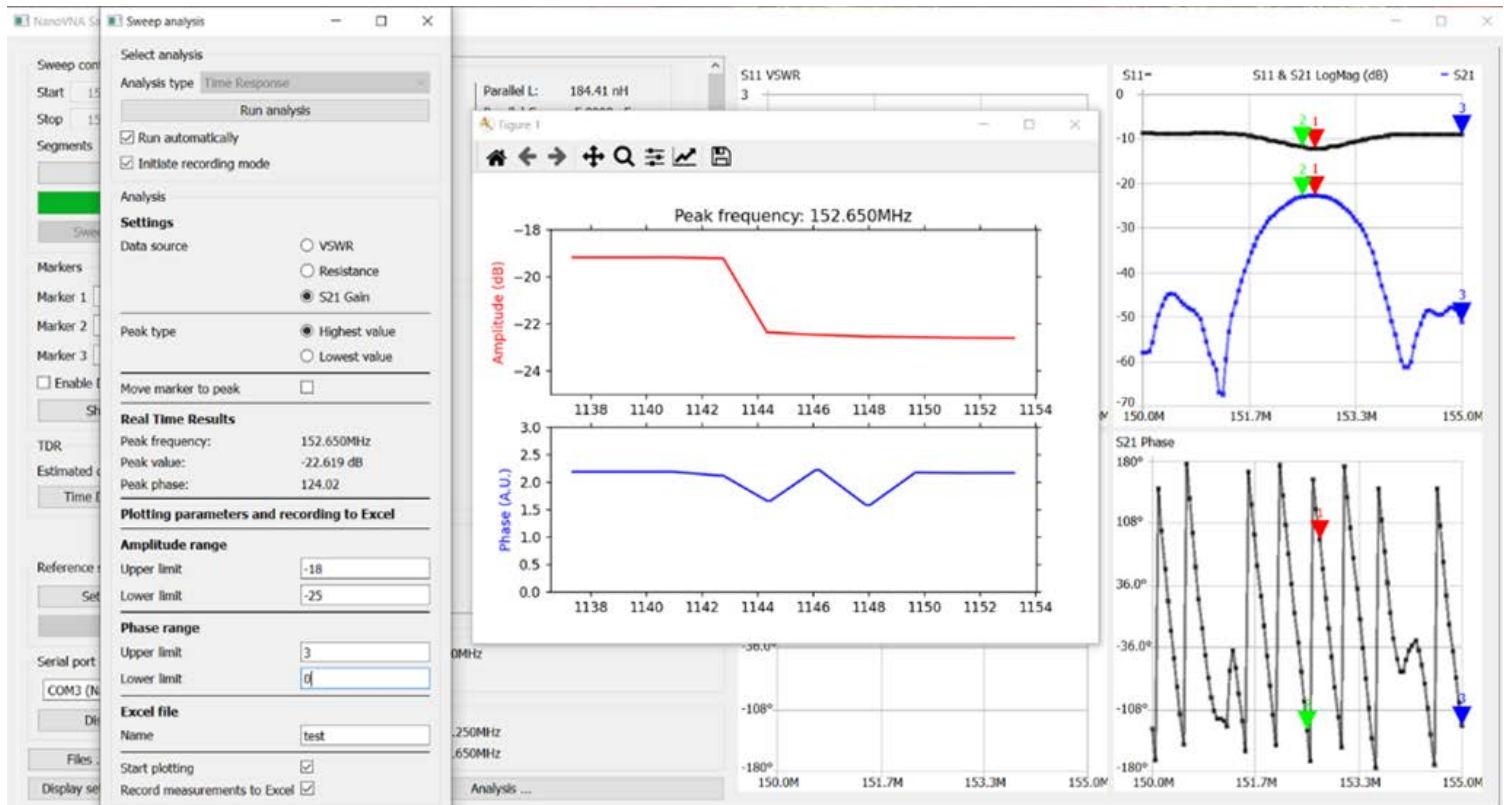


Fig. 2: NanoVNASaver software that was modified for the needs of real-time amplitude and phase measurements (red and blue lines, respectively)

3.4. Fabrication of the device holders and microfluidics

The first setup that was tested was previously described by Papadakis et al. (2018). Briefly, the microfluidic cards were created from 75 μm thick polyolefin foils structured by a CNC cutter and heat-laminated to a 6-layer stack in the micro-fluidics rapid-layer-manufacture service of Jobst Technologies GmbH, Germany. The contact between the SAW device and the microfluidic card was achieved by using ultra-narrow low loss seals (MED-6215 silicone, NuSil Technology LLC, USA) with less than 100 μm seal width and attached to the cards by using a precision milled PMMA mold. The polycarbonate docking station (Fig. 3a) was created by precision CNC machining and a seal made from MED-6215 was attached at the rear end of the station to provide the inlet and the outlets of the microfluidics. The docking station also houses two PCB boards that include the IPEX RF connectors and the probe pins in order to connect the SAW devices with the network analyzer.

The second setup was fabricated by using 1 mm thick PCB prototyping boards (Fig. 3b). Three pieces of the boards were used for the construction of the station and the copper layer of each board was grounded in order to minimize RF interference. The connection with the SAW device was achieved by using the same PCB boards that were used for the previous

docking station. The acoustic device was placed on a microscope slide with a patterned parafilm (Sigma-Aldrich) layer that acted as a guide, and then the slide was placed between the PCB boards to achieve the connection with the analyzer. The boards were held together by using neodymium magnets. The size/number/location of the magnets was optimized in order to minimize the insertion losses in air.

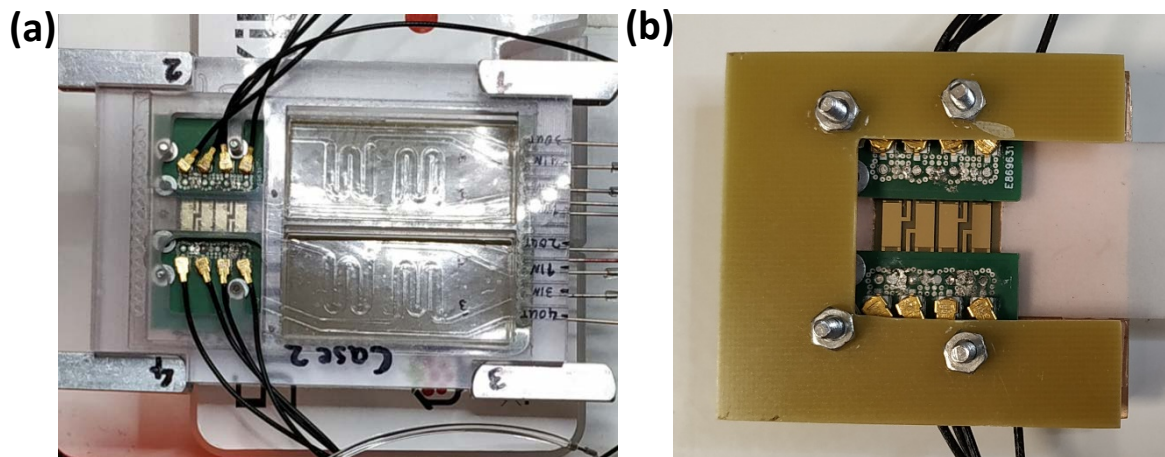


Fig. 3: (a) Polycarbonate docking station with microfluidic card and PCB heaters; (b) PCB prototype docking station.

3.5. LAMP amplification protocol

The LAMP amplification protocol was previously developed by Papadakis et al. (2018). Briefly, counted *Salmonella* cells resuspended in PBS buffer and lysed for 10 min at 95 °C. The invasion gene *invA* was targeted by a set of six primers (Chen et al., 2011), two outer (F3 and B3), two inner (FIP and BIP) and two loop (Loop-F and Loop-B). F3: CGGCCCGATTTTCTCTGG, B3: CGGCAATAGCGTCA-CCTT, FIP:GCGCGGCATCCGCATCAATATGCCCGGTAAACAGATG-AGT, BIP:GCGAACGGCGAAGCGTACTGTGCGCACCGTCAA-AGGAAC, Loop-F: GGCCTTCAAATC-GGCATCAAT, Loop-B: GAAAGGGAAAGCCAGCTTTACG. A primer mix with a total volume of 100 μ L was made and contained: 1.8 μ M (18 μ L) FIP and BIP, 0.1 μ M (2 μ L) F3 and B3, 0.4 μ M (6 μ L) Loop-F and Loop-B. The LAMP reagent mix has a total volume of 25 μ L and contained: 12.5 μ L WarmStart 2 \times colorine Master Mix (New England BioLabs), 2.5 μ L primer mix and 1 μ L lysed cells in PBS (or 1 μ L PBS for the control reaction). The minimum required time for successful DNA amplification from \sim 100 cells was 20 min at 63 °C.

3.6. Acoustic detection of LAMP products

Before each experiment, the SAW sensor surface was cleaned either by using deionized water and gently rubbing the surface with a cotton bud, or by etching the surface by using an air Plasma Cleaner/Sterilizer PDC-002 (Harrick Plasma Inc., Ithaca, NY, USA) instrument for 120 s at high RF level. The latter method was found to affect dramatically the operating frequency of the device, resulting in a frequency drift over the number of experiments (refer to section 4.3.).

Contrary to the acoustic detection protocol that was proposed by Papadakis et al. (2018), where the LAMP reactions (25 μ L total volume) were directly injected on the functionalized sensor surface, in the present experiments 20 μ L of each LAMP reaction (control and sample) was diluted in 980 μ L of 10mM Tris buffer with pH = 7.5. The purpose was to increase the amount of the available LAMP product volume in order to test the different setups with the same sample and to reduce the signal that comes from the absorption of molecules in the control reaction. Surface functionalization was performed by injecting 0.8 μ M of PLL-g-PEG (diluted in 10mM filtered Tris pH 7.5), followed by buffer rinsing until stabilization. The two LAMP reactions (control and sample) were subsequently injected and rinsed with buffer (respectively). All steps were performed at a flow rate of 20 μ L/min using a peristaltic micropump (Jobst Technologies GmbH). At the end of each experiment, the SAW device was cleaned as described before, while the polycarbonate docking station, the tubing and the pump were washed with 70% ethanol, 2% Hellmanex III (Hellma GmbH, Müllheim Germany), deionized water and dried under N₂ flow.

Chapter 4: Results and discussion

4.1. Device characterization and selection

Our initial aim was to assess the two different device substrates, quartz and lithium tantalate and evaluate their performance upon liquid loading. A major concern of selecting the proper type of device is the dielectric constant (DC) of the material in use. Most of the molecular biosensing applications require a liquid environment and it was estimated by Kaatz & Uhlendorf (1981) that the DC constant of water at the frequency band 0.1 - 114 GHz is approximately 78.32, at 25 °C. This value is much higher than the DC of quartz, which is approximately 4.5 at 20 °C (Bottom, 1972), leading to a high dielectric mismatch. As a result, when the devices come in contact with the water, the periodic high frequency electric fields that generated in the IDTs are shorted out (Länge et al., 2008). A way to overcome the aforementioned problem is the deposition of an insulating layer over the IDTs and the sensing area of the device (Hamidon & Yunusa, 2016). An alternative approach is to use substrate materials with higher DC. In the present study, LiTaO₃ was selected as a piezoelectric substrate for the SAW device that would compensate the high dielectric constant of the liquids under investigation. Lithium tantalate in the range of 0.5 – 100 MHz has a dielectric constant of 43 (stressed) and 45 (unstressed) (Warner, 1967). Therefore, because of the higher DC value of LiTaO₃, devices that use this substrate can potentially be used in applications that require the analysis of an aqueous solution, even when the device is completely immersed, without the need of depositing a protective/waveguide layer over the IDTs (Shiokawa & Moriizumi, 1988). Based on the aforementioned considerations, a comparison between the quartz and lithium tantalate devices was made. The devices were tested by using the polycarbonate docking station and a microfluidic card with 2 different fluidic channels that cover the sensing area of the array (Fig. 4a). The frequency range in the network analyzer was set from 140 to 157.8 MHz for both devices, lithium tantalate and quartz (Fig. 4b, c, respectively).

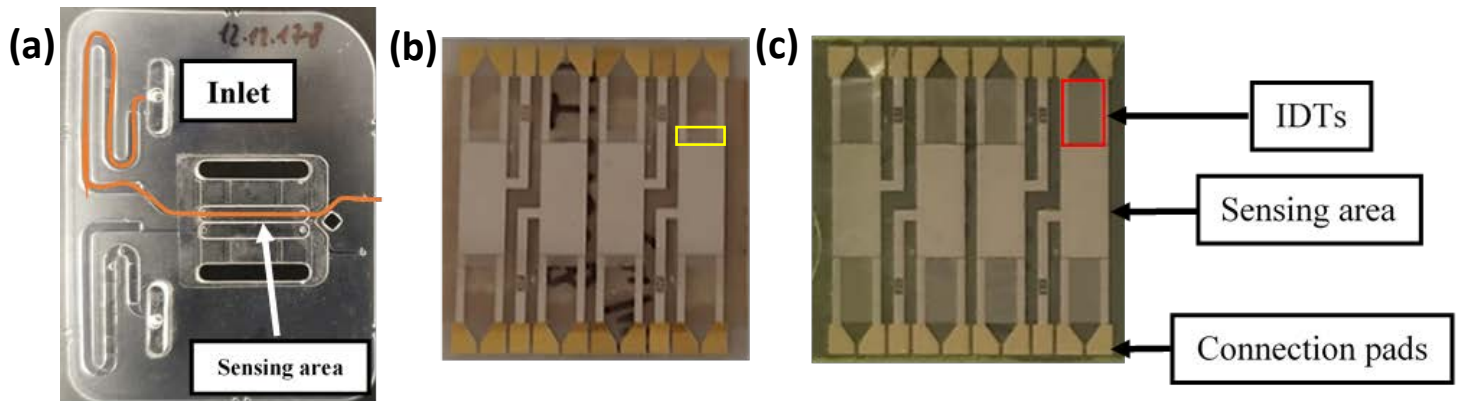


Fig. 4: (a) Microfluidic card with two channels and the path of the liquid inside the channel (orange line); (b) Lithium tantalate array at 155 MHz with interdigital transducers (IDTs) near the sensing area (yellow square); (c) Quartz array at 155 MHz with dense network of IDTs (red square).

The sweep response of both substrates in air was acceptable and as it is shown in Fig. 5, lithium tantalate had a wider bandwidth (Fig. 5a) compared to quartz (Fig. 5b). The narrow response of the latter it is known due to the low electromechanical coupling coefficient ($\sim 9\%$), compared to the higher coupling coefficient of LiTaO_3 ($\sim 40\%$), and as a result the bandwidth of the quartz devices is restricted near the fundamental working frequency (Hales & Burgess, 1976). Regarding the phase response of the two substrates, it is evident that in quartz the curve was linear, near the fundamental frequency, while in lithium tantalate random phase fluctuations occurred. The same pattern it was also observed in the amplitude response. Upon loading of liquid (water) in both microfluidic channels, in the case of the lithium tantalate device (Fig. 5c), the amplitude attenuated, while the phase and the amplitude became noisy over the whole spectrum. Quartz presented the same attenuation response for amplitude, however, as it is shown in Fig. 5d, both parameters retained their linearity and noisy immunity.

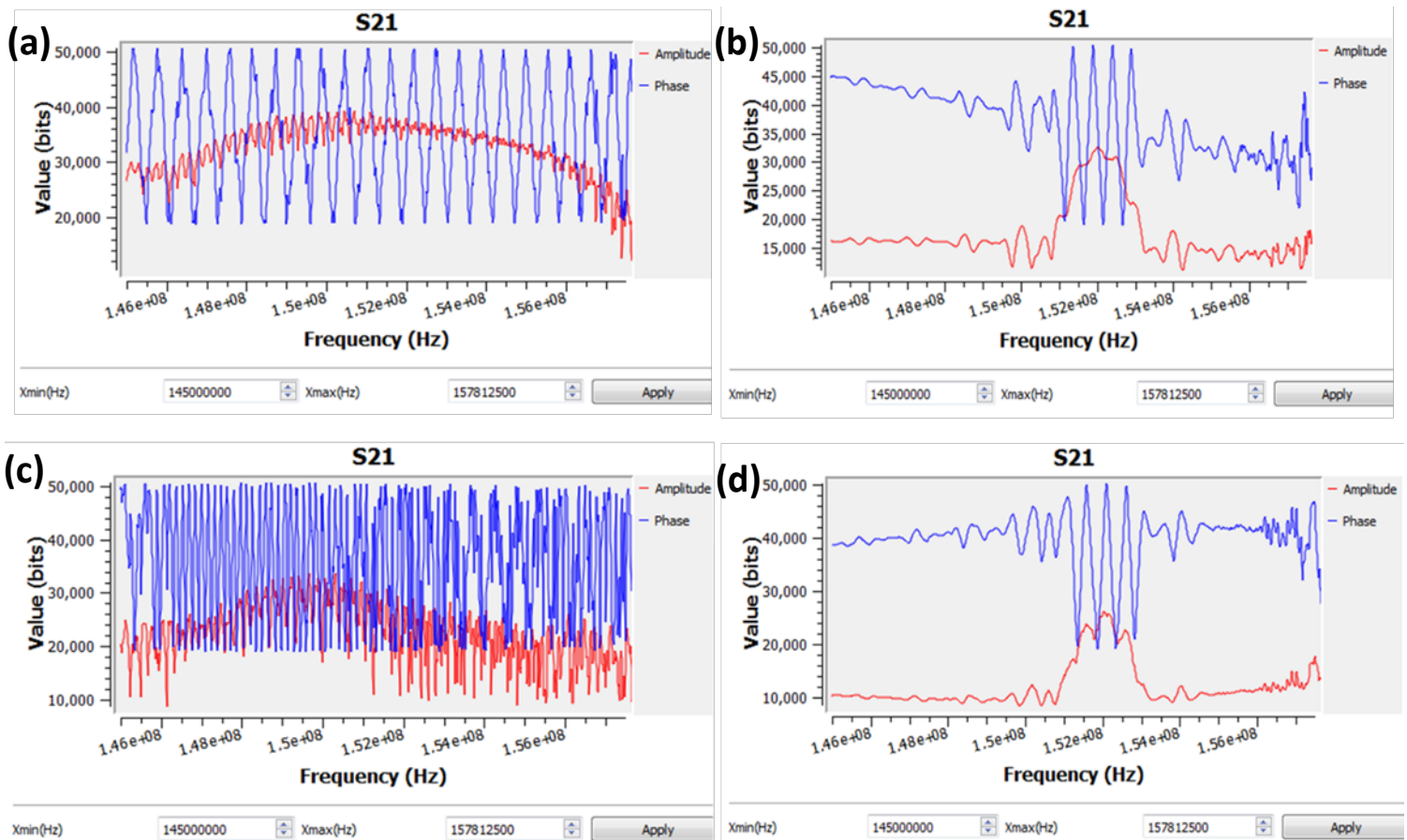


Fig. 5: Images of acoustic signal spectra: (a) Lithium tantalate in air; (b) Quartz in air; (c) Lithium tantalate with water filling the microfluidic card; (d) Quartz with water filling the microfluidic card.

A possible explanation for this response is the reflected waves on the surface of the device that caused by the high coupling coefficient of LiTaO_3 , and in order to test this hypothesis absorbers made from soft materials placed on the device in different arrangements. The best attenuation of noise was achieved by placing parafilm strips (12 x 2 mm) on both sides of the IDT lines. A similar configuration was also suggested by Jakoby & Vellekoop (1997). The parafilm strips (Fig. 6a) act as absorbers of the reflected waves and as a result they significantly reduce the spurious effects on both amplitude and phase in air (Fig. 6b). However, upon loading of liquid in the sensing area of the device, the spurious response was once again evident, even in the case of microfluidic cards that covered one channel of the array (Fig. 6c).

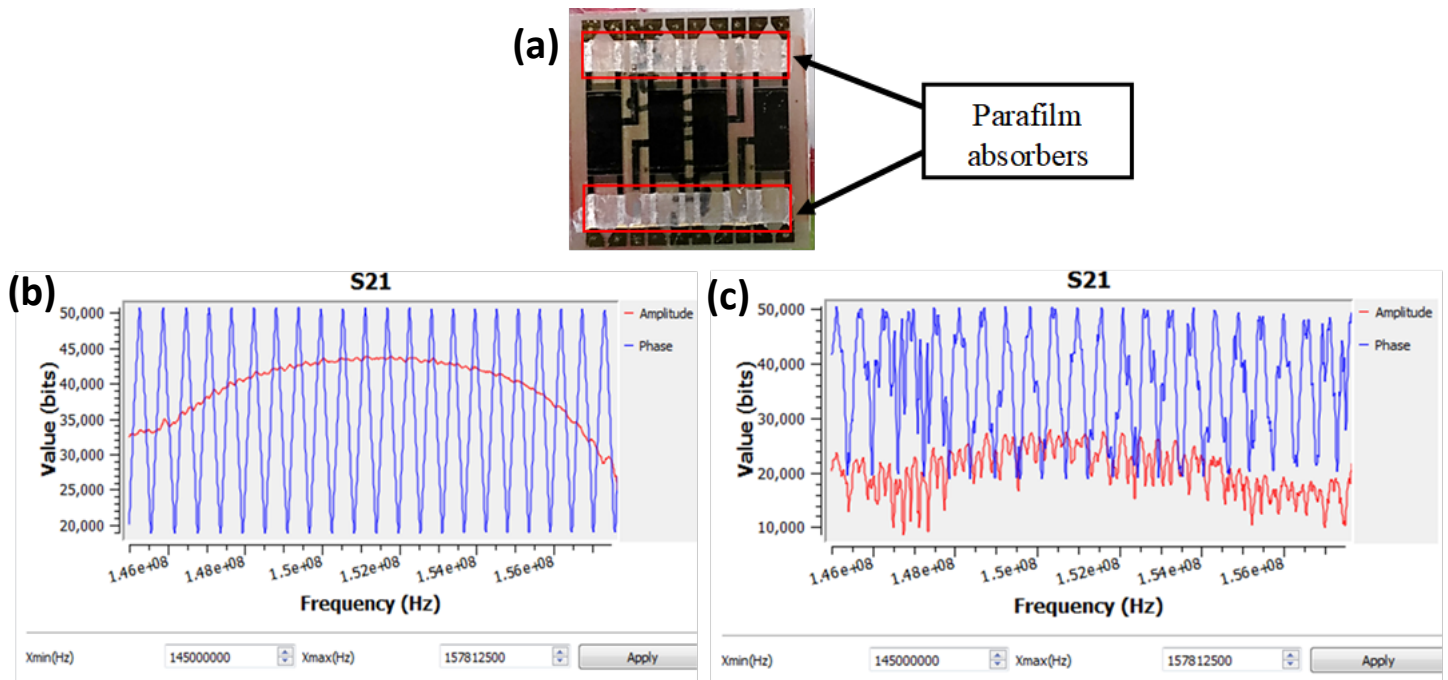


Fig. 6: (a) Lithium tantalate array with parafilm absorbers; (b) Lithium tantalate acoustic response with parafilm absorbers; (c) Lithium tantalate acoustic response with parafilm absorbers and water filling the microfluidic card.

4.2. Network analyzer and calibration of SAW devices

After the characterization of the two substrates, the next step was to evaluate the ability of the two different network analyzers to acquire the amplitude and phase changes upon loading of a viscous liquid. For this set of experiments, glycerol standards were prepared in different concentrations. This experiment is a standard approach for the evaluation of the acoustic response of an acoustic setup by monitoring the change of amplitude and phase over the different solutions that offer pure viscous loading on the sensor surface (Mitsakakis et al., 2009; Samarentsis et al., 2020). A typical experiment of glycerol standards acquisition is presented in Fig. 7. All sample solutions were injected with a peristaltic pump at a flow rate of 20 $\mu\text{L}/\text{min}$, while rinsing was done by injecting deionized water. The four different plots in Fig. 7, acquired by using the SENSEOR VNA, represent the amplitude and phase change over the time with respect to the concentrations of the viscous glycerol sample. Regarding the amplitude response, three channels of the array were able to detect the viscosity changes (i.e., IDT1, IDT2, IDT4), while IDT3 showed a limited response and spurious acquisition. Regarding the phase changes, in all four channels of the array, it was not possible to obtain any step response. As it was described earlier, the absence of phase linearity in the spectrum of lithium tantalate (Fig. 5c), creates the noisy effect on the acquisition of the phase signal.

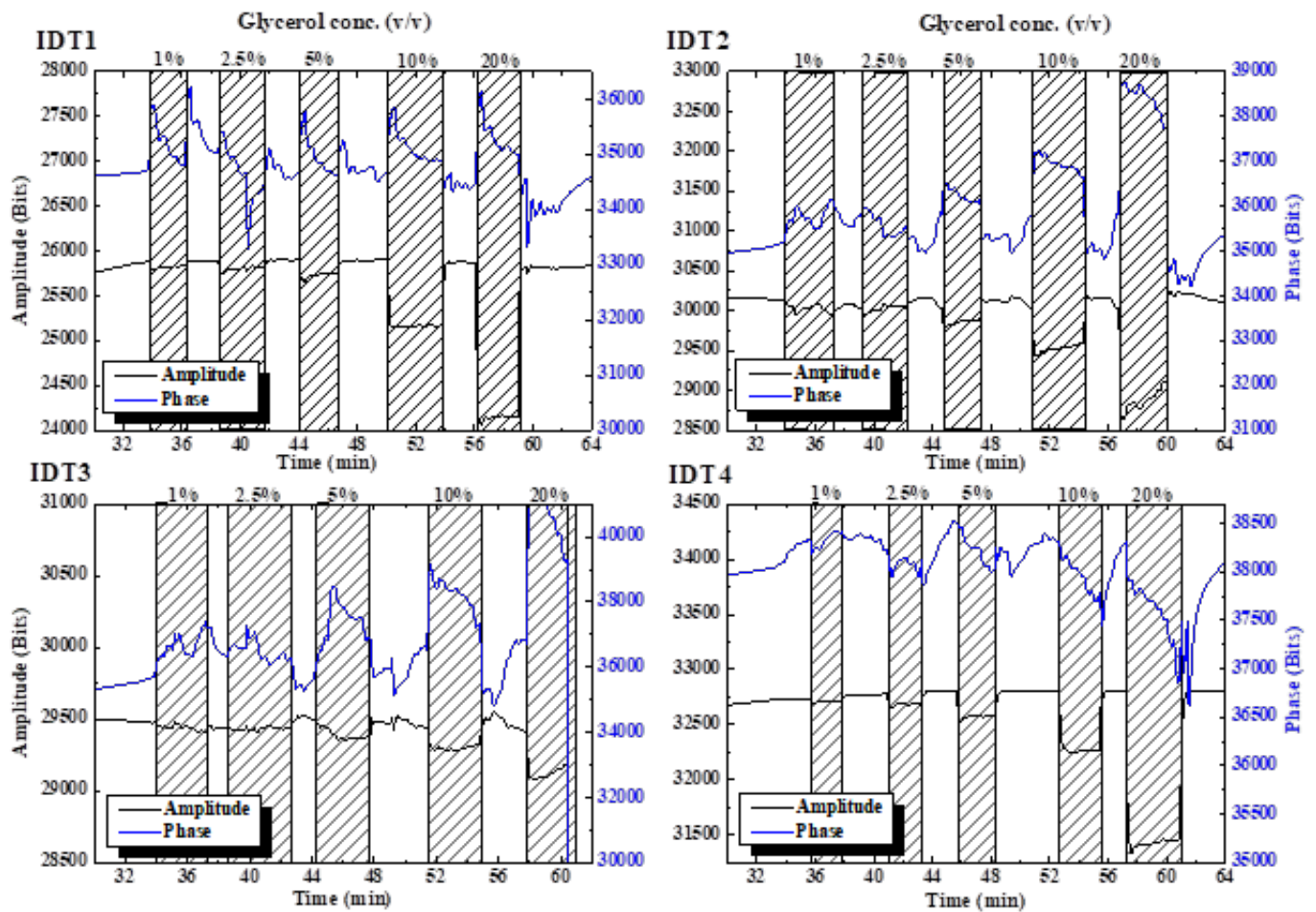


Fig. 7: Real-time representation of the acoustic wave amplitude and phase using a lithium tantalate device. Series of injections was as follows: 1, 2.5, 5, 10, 20% (v/v) glycerol. The blue and black lines correspond to changes in phase and amplitude, respectively. Both phase and amplitude are measured in bits.

In order to compare the two different VNA instruments and their ability to monitor the changes of the signal and in parallel to ensure that the phase noise is not a fault of the SENSEOR analyzer, the same experiment was repeated by using the NanoVNA. Figure 8 represents the comparison of the two instruments. For both devices the amplitude attenuation with respect to the glycerol concentration was linear ($R^2 > 0.97$ in all cases), indicating that both instruments can be used and discriminate the different concentrations of glycerol. The phase change cannot be recorded either with NanoVNA due to extended noise and spurious response. Although both instruments recorded the changes in the same scale, a different response of the same channels (i.e., IDTs) between the two experiments was observed. The reason of this deviation is attributed to the cleaning approach that was used and it was tested on the following section (i.e., 4.3.).

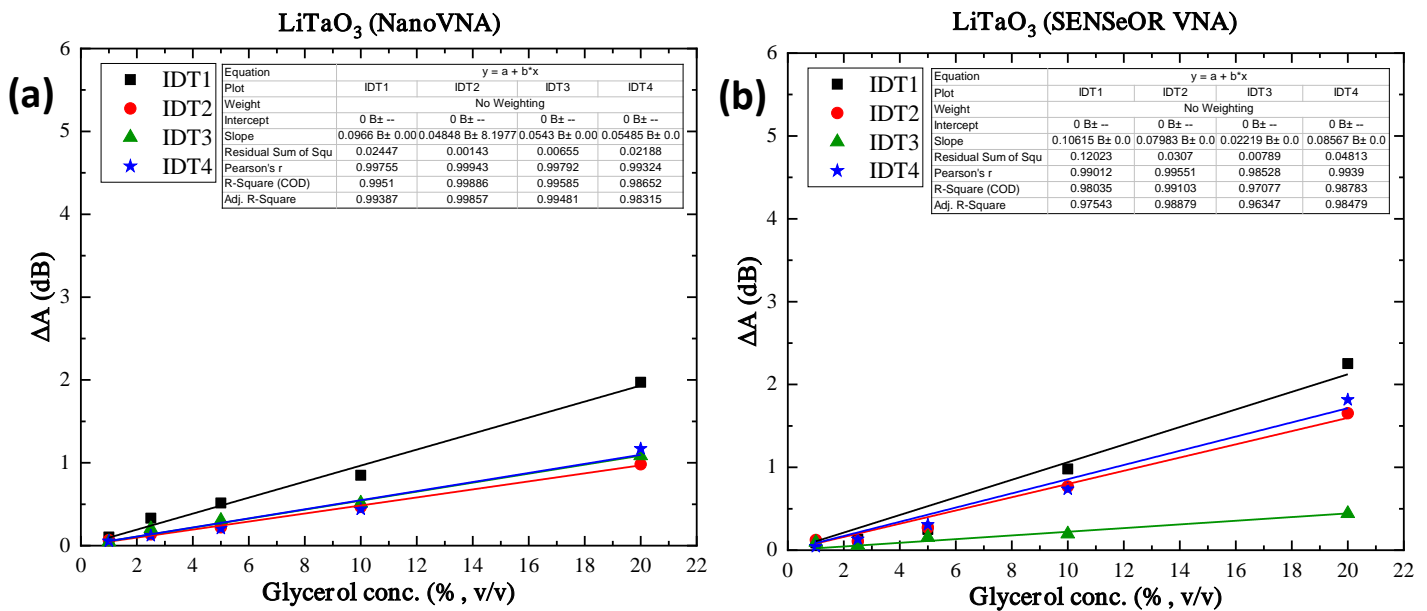


Fig. 8: Network analyzers comparison using a lithium tantalate device and glycerol calibration: (a) NanoVNA; (b) SENSEOR VNA.

Quartz substrates were also evaluated by performing the glycerol calibration experiment (Fig. 9). Each channel of the array was able to detect phase and amplitude changes, while the response of the phase was significantly better compared to that of lithium tantalate. Since glycerol solutions offer a viscous loading on the surface of the device, a change on amplitude with respect to glycerol concentration is expected (Saha et al., 2003; Tsortos et al., 2008; Mitsakakis et al., 2009).

Figure 10 shows the linear relationship ($R^2 > 0.99$ in all four channels) between the amplitude attenuation (ΔA) with respect to the glycerol concentration (v/v, %). During the washout of the sensor surface with water, the signal returns to its original baseline, indicating that the glycerol-water solution is properly rinsed off. As it is mentioned by Saha et al. (2003), since the glycerol mixture does not adsorb to the sensing surface, it is expected that the mass (phase change) is poorly sensed. From Fig. 9 it is evident that the phase response in the channels IDT1 and IDT2 is poorly sensed, while the opposite happens in the case of the channels IDT3 and IDT4, on which the relative change of phase (in bit units) is smaller compared to amplitude (in bit units).

By comparing the amplitude response upon viscous loading of the two different substrates (Fig. 8 and Fig. 10), it is evident that the quartz SAW devices are more sensitive compared to lithium tantalate due to the higher slope values of the trendlines (i.e., 0.24 in average for quartz vs 0.075 in average for lithium tantalate (Fig. 5b)). The results are in agreement with previous works (Mitsakakis et al., 2009; Samarentsis et al., 2020), therefore

for the molecular detection experiments and the development of the platform, quartz devices were selected.

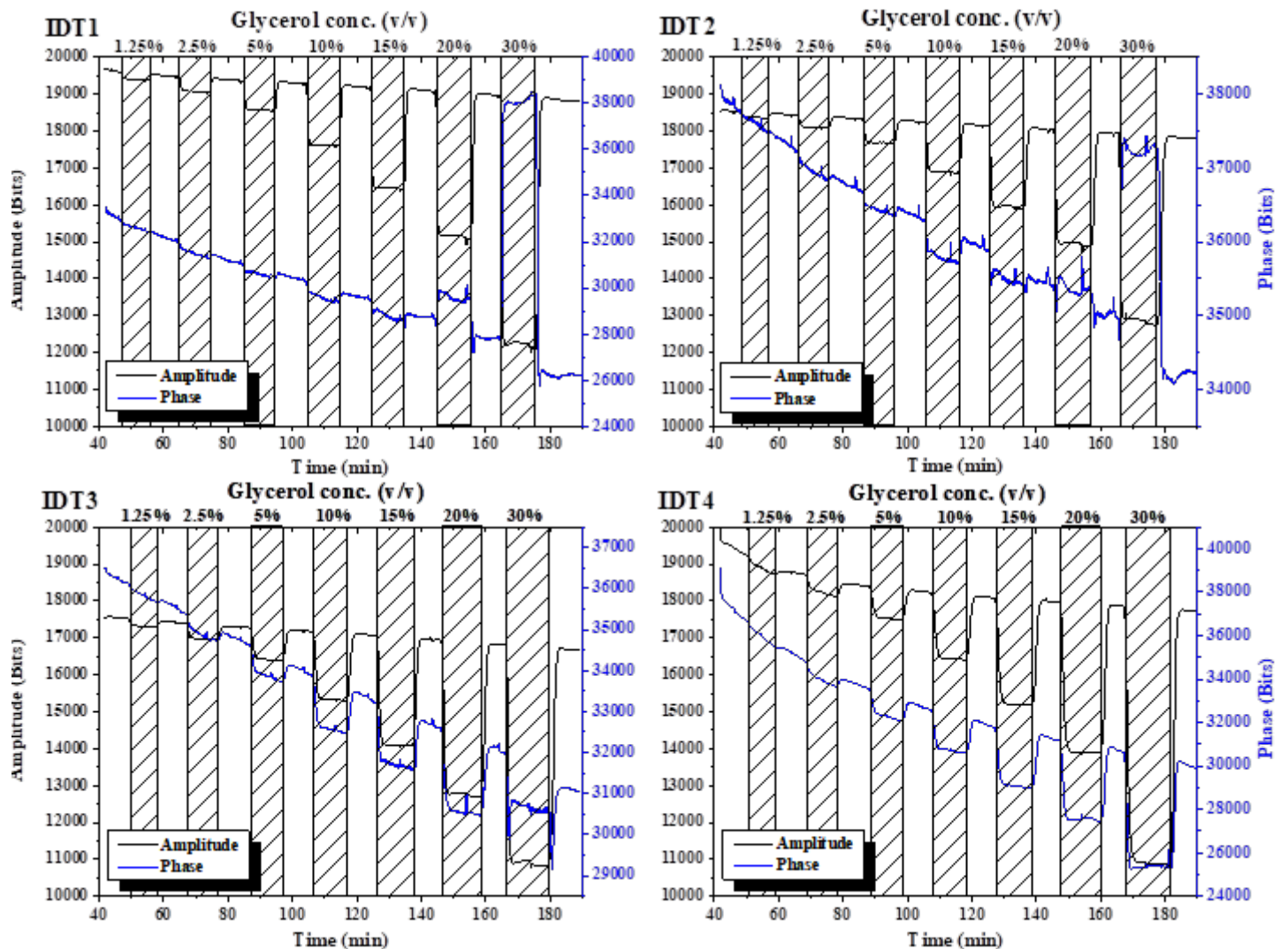


Fig. 9: Real-time representation of the acoustic wave amplitude and phase using a quartz device. Series of injections was as follows: 1.25, 2.5, 5, 10, 15, 20, and 30% (v/v) glycerol. The blue and black lines correspond to changes in phase and amplitude, respectively. Both phase and amplitude are measured in bits.

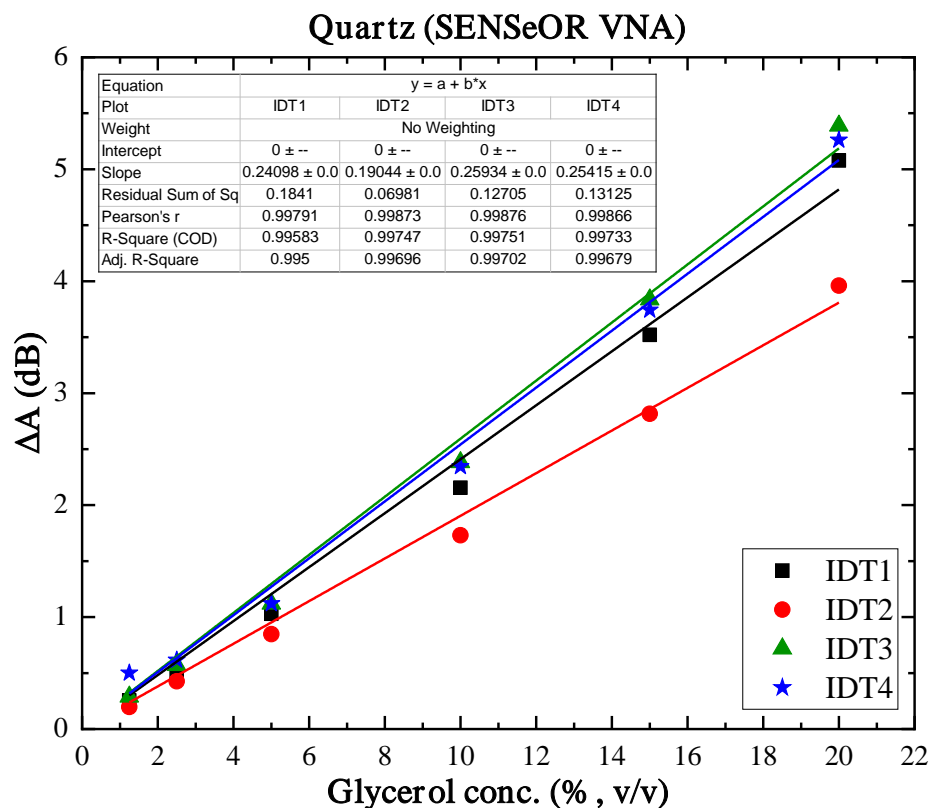


Fig. 10: Glycerol calibration of quartz device by using SENSeOR network analyzer.

4.3. Cleaning of the devices

A highly important parameter for the development of a portable and reliable SAW platform is the recycling/cleaning of the device after each test. Ideally, a device should last for a number of experiments in order to reduce the cost of the setup, and should be able to be recycled properly without the need for depositing a new layer of the waveguide each time. In the present study, several ways to clean the surface were tested. The waveguide of all the devices consists of a positive photoresist (S1813) which was found to be vulnerable to common detergents (e.g., Hellmanex 1%) and solvents like ethanol, isopropyl alcohol and acetone. Alternative cleaning methods have been suggested in the literature (Papadakis et al. 2017a, 2018), either by etching the surface with an air-plasma cleaner or by gently cleaning the device with a cotton bud. Previous studies have reported the importance of the waveguide layer and its thickness to the sensitivity of SAW devices. In fact, it was shown how the thickness of the applied waveguide layer and its properties affects considerably the response and the stability of amplitude and phase measurements (Du et al., 1996; Gizeli et al., 2003; Mitsakakis et al., 2009; Li et al., 2017; Papadakis et al., 2017a, 2018; Samarentsis et al., 2020).

Considering the limitation of a portable device that needs replacement of the device (or etching and deposition of new waveguide) each time, a set of experiments was carried out to evaluate the surface cleaning with cotton bud or air-plasma. For both cleaning methods used, the operational frequency of the device was observed over the course of the experiments. As it is shown in Fig. 11a, cleaning a quartz device with air-plasma, progressively results in a drift of the fundamental frequency towards higher values. That observation was valid for all four channels of array and progressively it was observed a degradation of the phase and amplitude curves with the presence of noise and spikes (data not shown). The opposite pattern was observed in the second set of experiments by cleaning the surface of a quartz device with a cotton bud (Fig. 11b). During the first four experiments a frequency drift was observed, however up to the 13th experiment the fundamental frequency remained relatively stable. After the 13th experiment, extensive wear of the device contact pads from the probe pins of the docking station resulted to poor electrical connections and the device was defective. Therefore, the method of cleaning the devices with a cotton bud is efficient, cost-effective method for the portable platform project, and the device can last up to 13 experiments without a concerning degradation of the acoustic parameters and sensitivity, which was evident in the case of air-plasma cleaning.

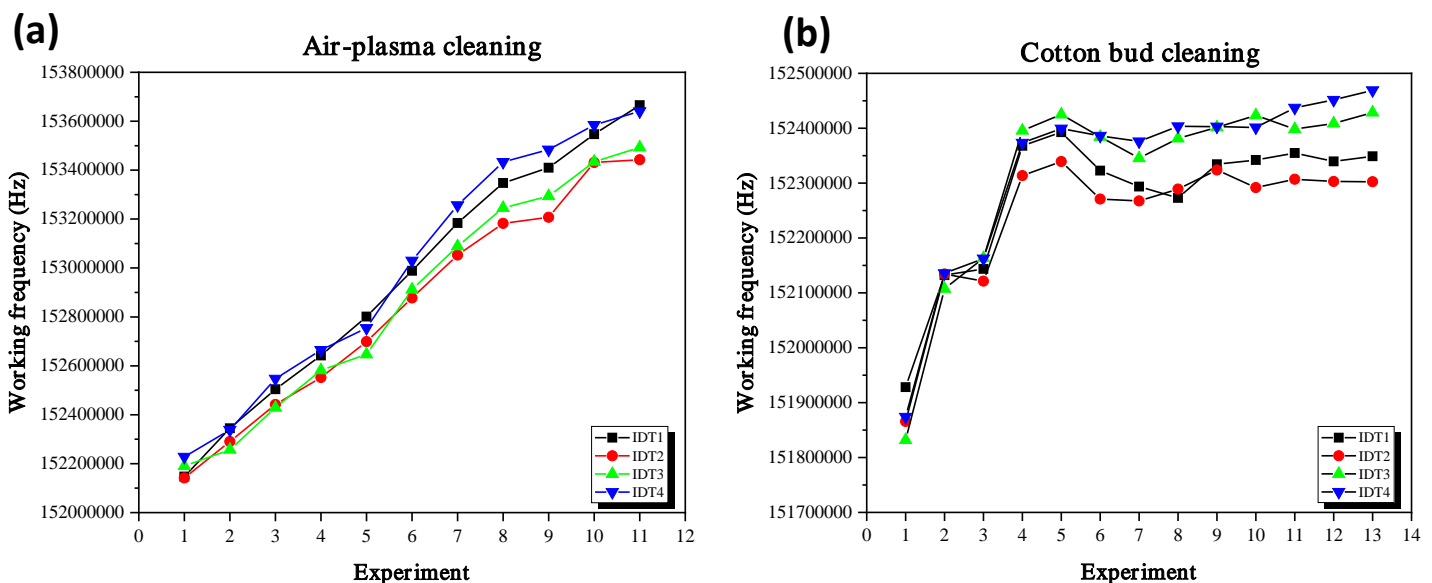


Fig. 11: Frequency drift of quartz devices over the number of experiments with two different cleaning methods: (a) air-plasma cleaning; (b) cotton bud cleaning.

4.4. Acoustic response evaluation and LAMP detection

The next step after the glycerol calibration and establishing the cleaning/reusing of the devices, was to evaluate the response of the setup to detect the binding of DNA amplified products by using the LAMP method. The loop-mediated isothermal amplification (LAMP) is a newly developed molecular technique for the amplification of molecular targets (i.e., genes). In contrast to the other DNA amplification methods, for example polymerase chain reaction (PCR), LAMP performs the amplification task under isothermal conditions, thus eliminating the need of a specialized thermocycler that varies the temperature of the reaction based on the amplification step. The LAMP method combines several advantages such as rapidity, high specificity due to the use of six gene regions and simplicity (Notomi et al., 2015), thus the use of such a molecular amplification approach is preferable for a portable detection platform since it eliminates the need of complex instrumentation and simple heating elements such as resistors or peltiers can be used, while it offers the opportunity to perform the reaction in the field without the need of laboratory facilities (Sirichaisinthop et al., 2011).

Different concentrations of the target, in this case *Salmonella* cells, were amplified using a thermocycler at the constant temperature of 63°C for 20 minutes. Prior to each measurement, functionalization of the sensor device took place by using PLL(25)-g-PEG(2), which results to greater acoustic shifts upon binding of DNA molecules, while it reduces the amount of non-specific binding of proteins (Papadakis et al., 2017b). Previous study that was conducted in our lab (Papadakis et al., 2018) showed that a similar setup has limit of detection of 50 cells for an amplification time of 30 minutes, while the results indicated that amplitude was more sensitive, than phase, to the differentiation between negative and positive samples. However, in their work, non-specific binding of the negative samples (control reactions) was evident and resulted to approximately 0.2 dB of attenuation. In the present study, an attempt to reduce the amount of non-specific interaction took place. In order to achieve that, the amplification time was reduced down to 20 minutes, while an extra step compared to the work of Papadakis et al., (2018) was the dilution of the final LAMP amplified product in Tris buffer solution in order to minimize the binding of molecular by-products at the functionalized sensor surface (Wachiralurpan et al., 2021).

An indicative signal acquisition experiment is presented in Fig. 12. Upon binding of PLL-g-PEG on the surface of the quartz sensor, both amplitude and phase changed, with the latter resulting in a greater shift (i.e., 1573 ± 85 bits) compared to the amplitude attenuation (i.e., 331.5 ± 97.8 bits). This observation indicates that PLL-g-PEG binds on the surface of sensor and results in a high mass-sensitive phase signal. The same pattern was observed during the injection of the LAMP positive sample where the electrostatic attraction between the negatively charged phosphate groups of the DNA molecules and the positively charged ϵ -amino groups of the poly-L-lysine molecule (Papadakis et al., 2017b) resulted in higher phase shift (423.5 ± 135.4) compared to amplitude attenuation (298.25 ± 81.8). Papadakis et al. (2018) suggested that amplitude measurements were more sensitive than phase for the

discrimination between positive and negative samples. However, in all the experiments of the present study negative LAMP reactions (LAMP(-) in Fig. 12) were not detectable either by amplitude or phase measurements. Therefore, the reduction of LAMP amplification time to 20 min and the dilution of the LAMP products into buffer solution, effectively reduced non-specific binding of molecular by-products. Also, either amplitude or phase measurements can be used for signal acquisition.

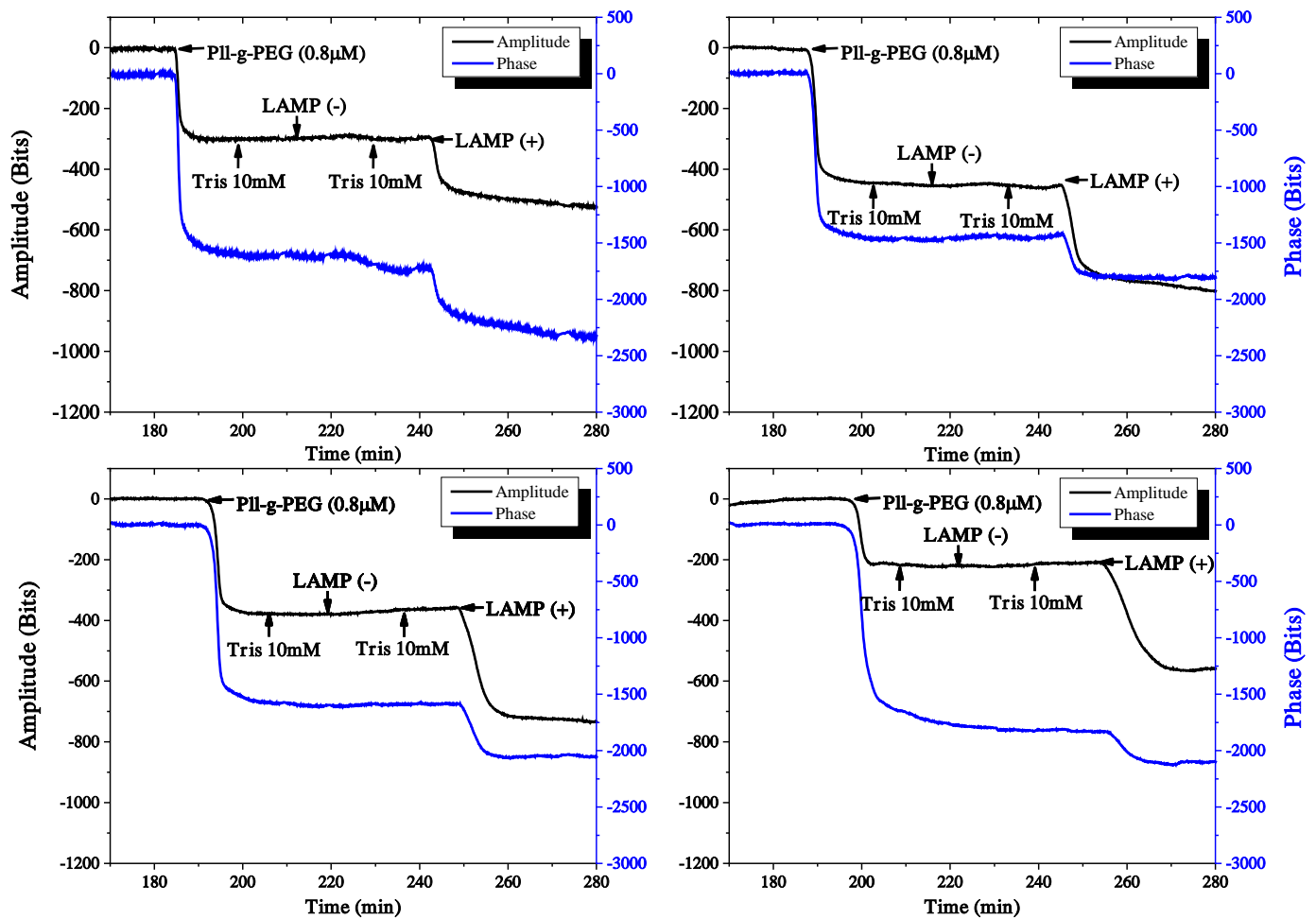


Fig. 12: Real-time binding curves of LAMP reactions flowing sequentially over the four different sensing areas of the array. The blue and black lines correspond to changes in phase and amplitude, respectively. Both phase and amplitude are measured in bits.

The final step was to evaluate the limit of detection (LoD) of the setup and compare the results of the presented methodology with the findings of Papadakis et al. (2018) study. Figure 13, presents the variation of amplitude change (ΔA , bits) with respect to the number of *Salmonella* cells that were present in the LAMP reaction. It is evident that the setup was able to detect down to 100 microbial cells. The higher concentrations of the target (i.e., 10^3 , 10^4 and 10^5 *Salmonella* cells), resulted to similar amplitude attenuation values (i.e., 291.8 bits or 0.38 dB in average), indicating that above the limit of detection of 100 cells, the setup reaches its upper detection threshold due to the saturation of the sensor's surface with DNA molecules. Interestingly, similar values (in dBs) for the positive LAMP reactions and observations were obtained by Papadakis et al. (2018), indicating that the approach of reducing the amplification time to 20 minutes and diluting the LAMP reactions is an effective strategy to eliminate the threshold that is required in order to distinguish the negative from the positive samples. However, from Fig. 13 it is observed that the error of amplitude attenuation measurements for the case of 100 cells is higher compared to the other cell concentrations. Papadakis et al., (2018) showed that their setup was able to detect the presence of approximately 50 cells in the LAMP reactions, but similarly to the present study, the error of the measurements for the case of low microbial concentrations was increased compared to samples with higher concentrations of *Salmonella* cells. A possible explanation lies with the fact that the four different microfluidic channels that covered each channel of the device/array, were connected in series, meaning that the outlet of the first microfluidic channel was the inlet for the next one. Therefore, the DNA molecules that do not bound on the sensing area of the first channel, due to the saturation of the surface, will be captured on the functionalized surfaces of the subsequent channels. However, in the case of low concentration of bacterial cells (i.e., 100 *Salmonella* cells), as it is depicted in Fig. 14, due to the reduced amount of DNA molecules in the injected sample, progressively less DNA molecules interacted with the functionalized surface of each channel, resulting in a progressively reduced amplitude change.

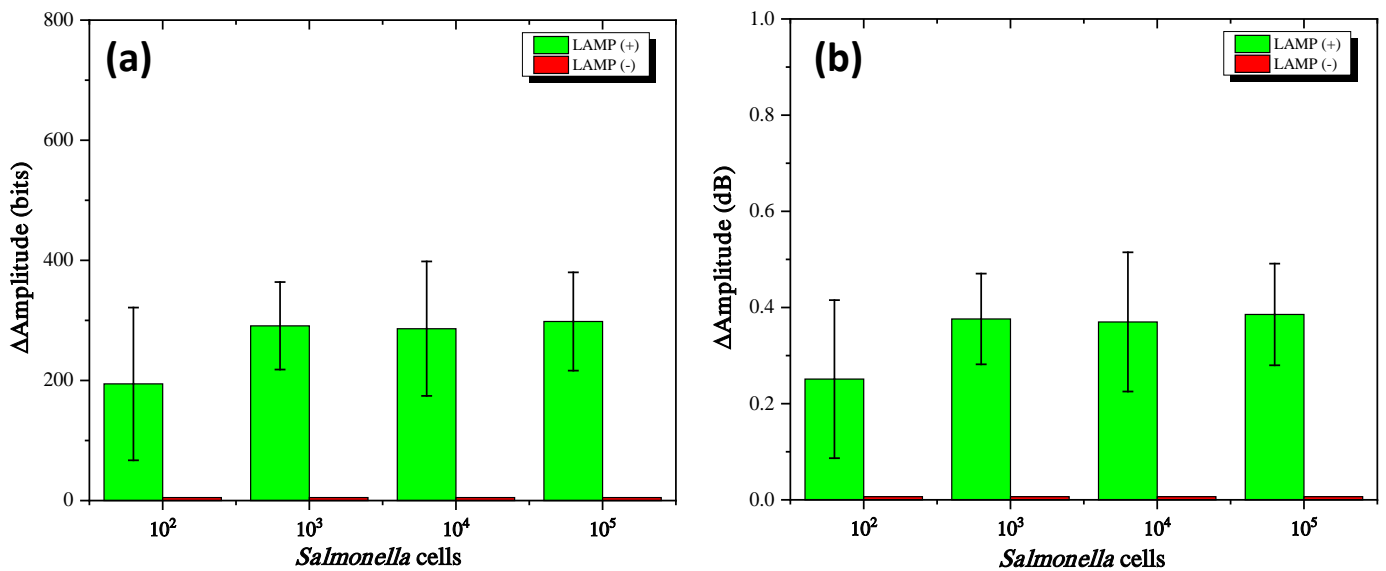


Fig. 13: Amplitude attenuation obtained during the detection of dsDNA amplicons produced during LAMP of 100, 10³, 10⁴, 10⁵ Salmonella cells (positive, green bars) and samples containing no cells (negative, red bars) using an acoustic waveguide device functionalized with PLL(25)-g[3.5]-PEG(2); (a) ΔAmplitude in bits; (b) ΔAmplitude in dB

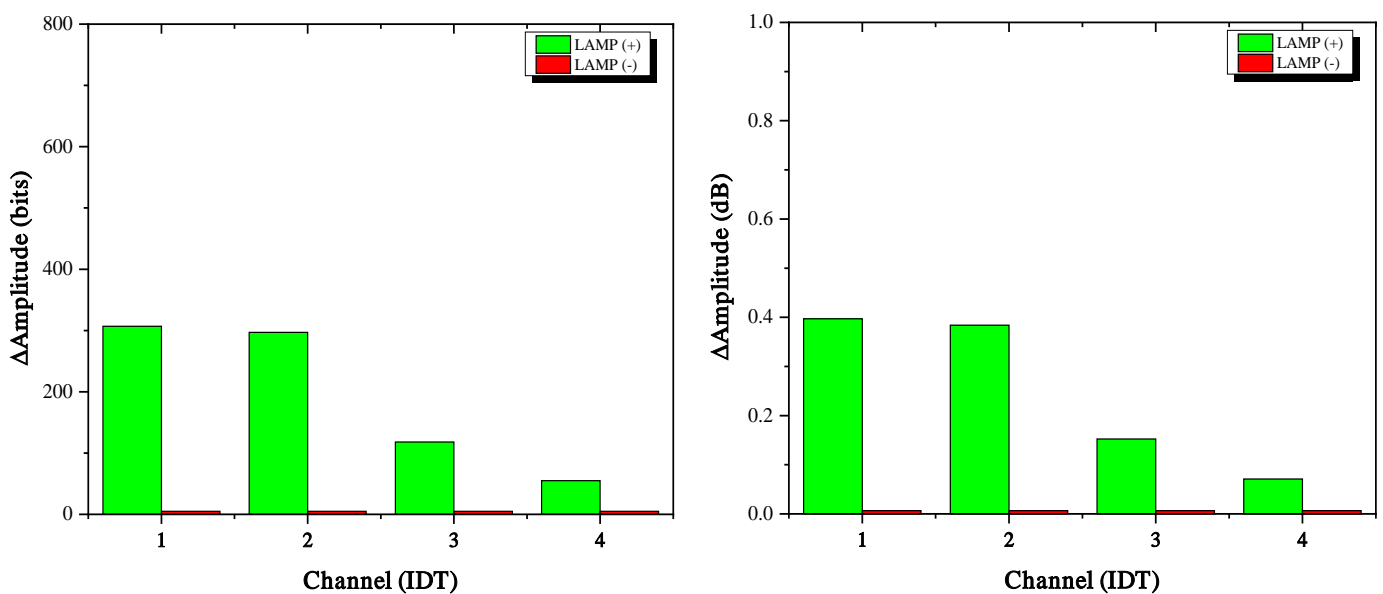


Fig. 14: Amplitude attenuation of each channel of the acoustic device (i.e., IDT) during the detection of dsDNA amplicons produced from LAMP reaction with 100 Salmonella cells (positive, green bars) and samples containing no cells (negative, red bars) using an acoustic waveguide device functionalized with PLL(25)-g[3.5]-PEG(2); (a) ΔAmplitude in bits; (b) ΔAmplitude in dB.

4.5. Lab-made docking station and low-cost microfluidics

An important aspect of the present study was the optimization and miniaturization of the microfluidic setup in order to develop a portable acoustic platform for the rapid detection of molecular targets. The first step was the construction of low-cost microfluidics by implementing commonly used and widely available materials. As it was previously highlighted by previous studies (Gronewold, 2007; Jo & Guldiken 2014; Papadakis et al., 2017a; Stoukatch et al., 2021), the construction of the proper microfluidic system possesses a great challenge for SAW sensors. The binding efficiency of molecules and the course of binding kinetics can be affected, resulting in possible deviations from the true results (Gronewold, 2007). Also, by placing a microfluidic module on the sensing area of the device, the signal is attenuated resulting in reduced sensitivity and increased background noise. Finally, a significant limitation is the cost for manufacturing a microfluidic device (Jo & Guldiken 2014), while recently it was proposed an interesting approach by using a low-cost solution that implements micromachining and does not require a cleanroom for the fabrication (Nguyen et al., 2017).

A common rule of thumb for fabricating microfluidics suitable for SAW devices, is the reduction of the side wall thickness that come in contact with the sensing area (Mitsakakis et al., 2008; Jo & Guldiken 2014; Papadakis et al., 2017a) and the use of soft materials (Papadakis et al., 2017a). In an attempt to fabricate an alternative microfluidic design based on the aforementioned rules, different prototypes were made by using a polycarbonate sheet (2 mm thick) and different sealing materials. As it is depicted in Fig. 15, a microfluidic seal made from parafilm was made, either by placing a thick gasket (Fig. 15a, d) or by placing a thin parafilm gasket (Fig. 15b) above the sensing area, even using a 200nm double sided tape (Fig. 15c).

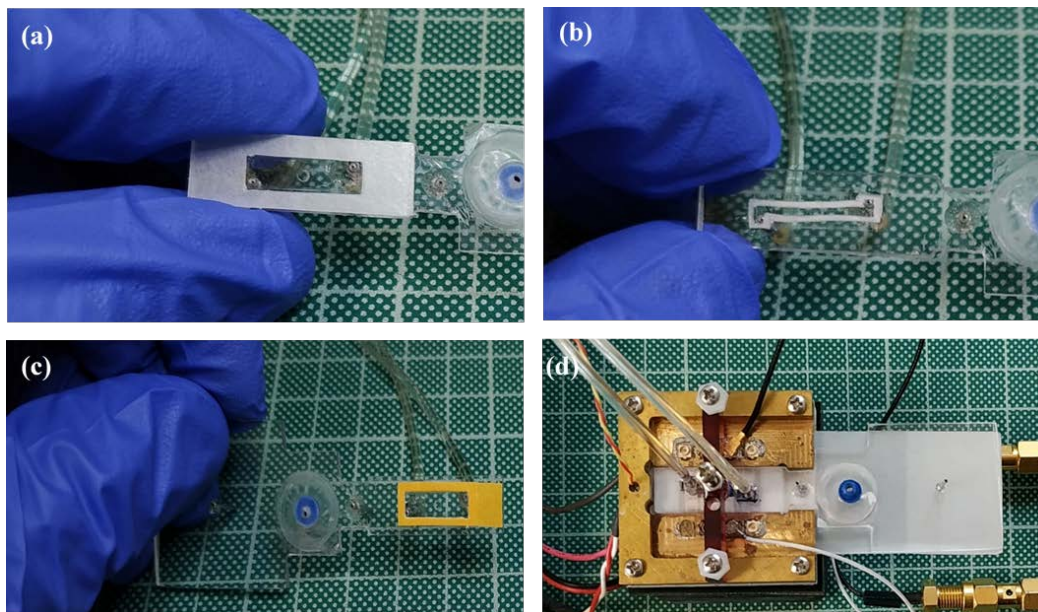


Fig. 15: Microfluidic gasket prototypes placed in a polycarbonate sheet with drilled inlets and outlets (metal pins): (a) thick parafilm gasket; (b) thin parafilm gasket; (c) double-sided tape; (d) brass docking station with parafilm gasket. The blue valve in the polycarbonate sheet was intended as bubble bleeder for future use.

For the gasket optimization experiments two different docking stations were tested, the first one was made by a brass base and the pressure could be adjusted by twisting seven different bolts (Fig. 16a) and the second docking station was made from PCB boards (Fig. 16b), while the pressure could be adjusted by varying the number/size/position of neodymium magnets. Several attempts were done with both configurations and the different parafilm gaskets, however leakage or strong attenuation problems were evident in all cases. Finally, the aforementioned setups were also tested with LiTaO₃ devices that based on bibliography are able to operate even when they are completely immersed in an aqueous solution (Shiokawa & Moriizumi, 1988), however even with a wide parafilm gasket that included the IDTs in the microfluidic channel, the signal was completely attenuated (Fig. 16c).

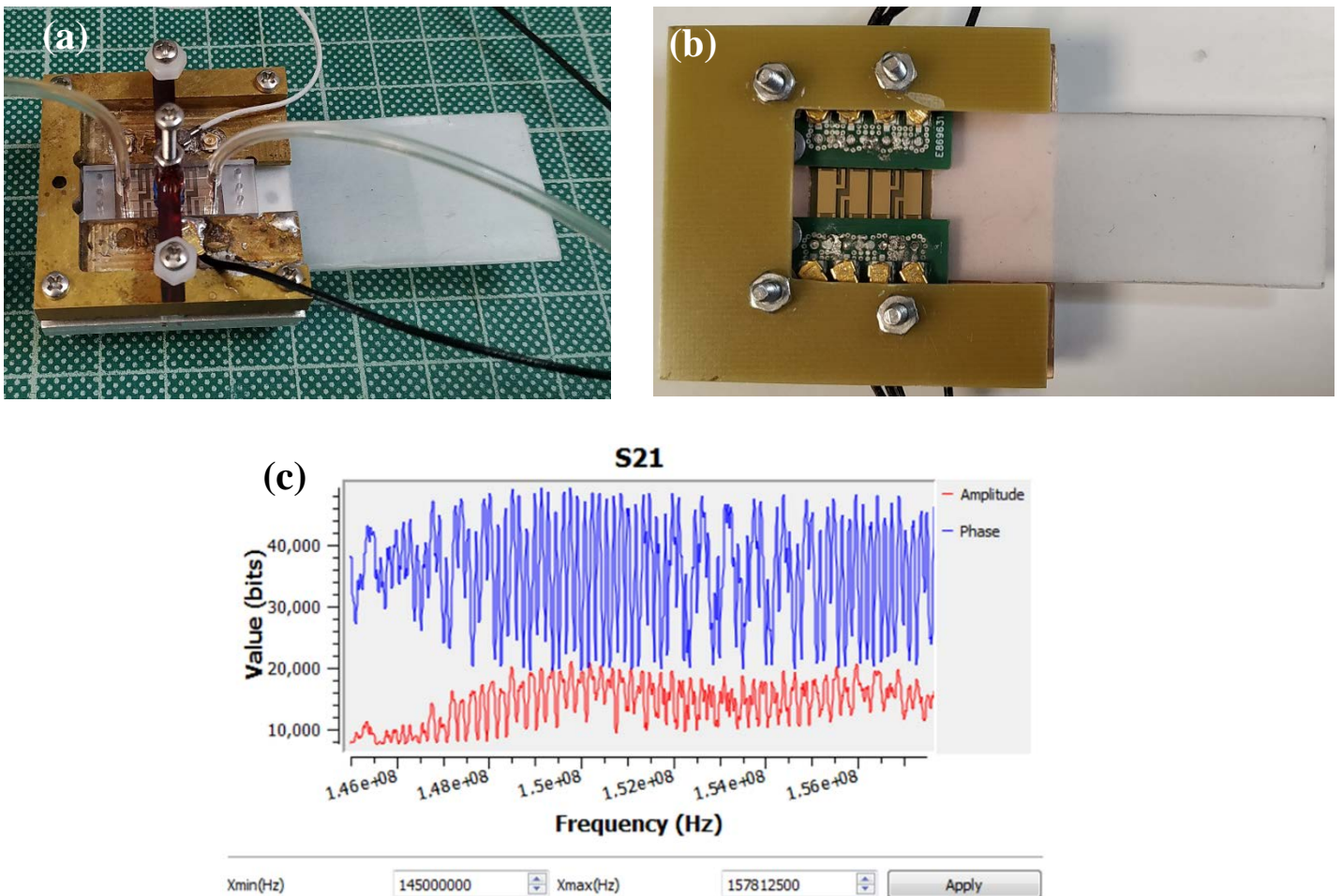


Fig. 16: Docking station prototypes: (a) brass made base with adjustable pressure mechanism; (b) PCB docking station with neodymium magnets. In both cases, the SAW device was placed on a microscope slide patterned with parafilm window for the device. (c) Lithium tantalate response with the thick parafilm microfluidic gasket.

Chapter 5: Conclusions

The current work demonstrates the crucial parameters and concerns for the development of an acoustic platform. Each aspect of the system should be carefully designed and evaluated in order to increase the overall cost efficiency and sensitivity of the setup. As it was shown, apart from the detection of the molecular target, several technical limitations take place upon the optimization of the platform.

Starting from the evaluation of the two available piezoelectric substrates, we consider that quartz devices are more suitable than lithium tantalate for the development of the prototype. Since the current lithium tantalate devices show a noisy response, further optimization of the waveguide material properties and thickness should be done. According to previous works (Shiokawa & Moriizumi, 1988; Trivedi & Nemade, 2017; Rana et al., 2018) the high electromechanical coupling coefficient of the aforementioned substrate is ideal for measurements in liquid media. Therefore, upon the establishment of a steady platform, we suggest that lithium tantalate should be considered as an alternative choice to quartz devices.

Regarding the microfluidic fabrication methods, as it was previously stated by Papadakis et al. (2017a) the application of acoustic sensors in LOC platforms as the biosensing element is still in the early stages of development due to the difficulties related to the SAW device integration with the fluidics and the device high sensitivity to several parameters. In the present, we focused to the integration of simple lab-made and low-cost microfluidic prototypes. However, we were not able to achieve a successful design and proceed with further experimental handlings. Therefore, the integration of fluidics in the surface of the sensor requires microfabrication solutions that potentially will increase the cost of the platform. Thus, we suggest that future investigation should mainly focus to alternative solutions for introducing the samples on the sensing area.

Finally, an also important parameter for developing a portable platform is the simplification and miniaturization of the signal acquisition instrumentation. The work of Nguyen et al. (2017) focused on the development of portable device capable to obtain sensitive measurements by monitoring the impedance changes of one-port acoustic devices, therefore they were able to significantly reduce the need of bulky and expensive VNA instrumentation. In this work we were able to test the ability of a hand-held and low-cost VNA analyzer to monitor amplitude and phase changes. We consider the specific instrument as an interesting tool to be integrated as a signal acquisition unit into the platform and we suggest that further development can be done in this direction.

To conclude, the development of an acoustic platform that can find application near the end-user has numerous challenges. Such a device should be reusable, reliable, sensitive, easy to handle, versatile and available to remote areas with low-cost. Throughout this work possible solutions to the limitations of SAW sensors are suggested and future research will focus mainly on alternative approaches to introduce the samples into the sensor. It is crucial

to eliminate the use of microfluidics which require high precision and expertise, while it is also highly important to minimize and simplify the instrumentation and the docking station. Ultimately, we consider that a viable and useful platform should consider the aforementioned criteria in order to find applications near the patient and in resource-poor settings.

References

- Aigner, R. (2008). Saw and BAW Technologies for RF filter applications: A review of the relative strengths and weaknesses. 2008 IEEE Ultrasonics Symposium. <https://doi.org/10.1109/ultsym.2008.0140>
- Alassi, A., Benammar, M., & Brett, D. (2017). Quartz Crystal Microbalance Electronic Interfacing Systems: A Review. *Sensors (Basel, Switzerland)*, 17(12), 2799. <https://doi.org/10.3390/s17122799>
- Andle, J. C., Vetelino, J. F., Lade, M. W., & McAllister, D. J. (1991). An acoustic plate mode device for biosensor applications. *TRANSDUCERS '91: 1991 International Conference on Solid-State Sensors and Actuators. Digest of Technical Papers.* <https://doi.org/10.1109/sensor.1991.148917>
- Ang, W. L., Lim, R. R., Ambrosi, A., & Bonanni, A. (2022). Rapid electrochemical detection of COVID-19 genomic sequence with dual-function graphene nanocolloids based biosensor. *FlatChem*, 32, 100336. <https://doi.org/10.1016/j.flatc.2022.100336>
- Bahadır, E. B., & Sezgintürk, M. K. (2016). A review on impedimetric biosensors. *Artificial cells, nanomedicine, and biotechnology*, 44(1), 248–262. <https://doi.org/10.3109/21691401.2014.942456>
- Balsam, J., Ossandon, M., Bruck, H. A., Lubensky, I., & Rasooly, A. (2013). Low-cost technologies for medical diagnostics in low-resource settings. *Expert Opinion on Medical Diagnostics*, 7(3), 243–255. <https://doi.org/10.1517/17530059.2013.767796>
- Balysheva, O.L. (2019). SAW Filters for Mobile Communications: Achievements and Prospects. *2019 Wave Electronics and its Application in Information and Telecommunication Systems (WECONF)*, 1-4. <https://doi.org/10.1109/WECONF.2019.8840661>
- Berlincourt, D. (1971). Piezoelectric Crystals and Ceramics. *Ultrasonic Transducer Materials*, 63–124. https://doi.org/10.1007/978-1-4757-0468-6_2
- Bhalla, N., Jolly, P., Formisano, N., & Estrela, P. (2016). Introduction to biosensors. *Essays in biochemistry*, 60(1), 1–8. <https://doi.org/10.1042/EBC20150001>
- Bottom, V. E. (1972). Dielectric constants of Quartz. *Journal of Applied Physics*, 43(4), 1493–1495. <https://doi.org/10.1063/1.1661347>
- Branch, D., Hayes, D., & Ricken, J. (2020). Handheld biosensor for COVID-19 screening. *Sandia National Laboratories.* <https://doi.org/10.2172/1671376>

- Bristol, T. W., Jones, W. R., Snow, P. B., & Smith, W. R. (1972). Applications of double electrodes in acoustic surface wave device design. 1972 Ultrasonics Symposium. <https://doi.org/10.1109/ultsym.1972.196097>
- Caliendo, C., & Hamidullah, M. (2019). Guided Acoustic wave sensors for liquid environments. *Journal of Physics D: Applied Physics*. <https://doi.org/10.1088/1361-6463/aafd0b>
- Chen, C., & Wang, J. (2020). Optical Biosensors: an exhaustive and comprehensive review. *The Analyst*. <https://doi.org/10.1039/c9an01998g>
- Chen, S., Wang, F., Beaulieu, J. C., Stein, R. E., & Ge, B. (2011). Rapid detection of viable *salmonellae* in produce by coupling propidium monoazide with loop-mediated isothermal amplification. *Applied and Environmental Microbiology*, 77(12), 4008–4016. <https://doi.org/10.1128/aem.00354-11>
- Chorsi, M. T., Curry, E. J., Chorsi, H. T., Das, R., Baroody, J., Purohit, P. K., Ilies, H., & Nguyen, T. D. (2018). Piezoelectric biomaterials for sensors and actuators. *Advanced Materials*, 31(1), 1802084. <https://doi.org/10.1002/adma.201802084>
- Clark, L. C., Jr, & Lyons, C. (1962). Electrode systems for continuous monitoring in cardiovascular surgery. *Annals of the New York Academy of Sciences*, 102, 29–45. <https://doi.org/10.1111/j.1749-6632.1962.tb13623.x>
- Cole, L. A. (2012). The hCG assay or pregnancy test. *Clinical Chemistry and Laboratory Medicine*, 50(4). <https://doi.org/10.1515/cclm.2011.808>
- Cremer, M. (1906). Über die ursache der elektromotorischen eigenschaften der gewebe, zugleich ein beitrag zur lehre von polyphasischen elektrolytketten. *Z. Biol.*, 47, 562–608.
- Damborský, P., Švitel, J., & Katrlík, J. (2016). Optical biosensors. *Essays in Biochemistry*, 60(1), 91–100. <https://doi.org/10.1042/ebc20150010>
- De Vicente, J., Lavín, Á., Holgado, M., Laguna, M. F., Casquel, R., Santamaría, B., Quintero, S., Hernández, A. L., & Ramírez, Y. (2020). The uncertainty and limit of detection in biosensors from immunoassays. *Measurement Science and Technology*, 31(4), 044004. <https://doi.org/10.1088/1361-6501/ab49ec>
- Depold, A., Erhardt, S., Weigel, R., & Lurz, F. (2021). A 10 khz to 6 ghz low-cost Vector Network Analyzer. *Advances in Radio Science*, 19, 17–22. <https://doi.org/10.5194/ars-19-17-2021>
- Devkota, J., Ohodnicki, P., & Greve, D. (2017). SAW Sensors for Chemical Vapors and Gases. *Sensors*, 17(4), 801. MDPI AG. <http://dx.doi.org/10.3390/s17040801>
- Di Nardo, F., Chiarello, M., Cavalera, S., Baggiani, C., & Anfossi, L. (2021). Ten Years of Lateral Flow Immunoassay Technique Applications: Trends, Challenges and Future Perspectives. *Sensors*, 21(15), 5185. MDPI AG. <http://dx.doi.org/10.3390/s21155185>

Ding, J., & Qin, W. (2020). Recent advances in potentiometric biosensors. *TrAC Trends in Analytical Chemistry*, 115803. <https://doi.org/10.1016/j.trac.2019.115803>

Ding, X., Peng, Z., Lin, S.-C. S., Geri, M., Li, S., Li, P., Chen, Y., Dao, M., Suresh, S., & Huang, T. J. (2014). Cell separation using tilted-angle standing surface acoustic waves. *Proceedings of the National Academy of Sciences*, 111(36), 12992–12997. <https://doi.org/10.1073/pnas.1413325111>

Drafts, B. (2001). Acoustic wave technology sensors. *IEEE Transactions on Microwave Theory and Techniques*, 49(4), 795–802. <https://doi.org/10.1109/22.915466>

Du, J., Harding, G. L., Ogilvy, J. A., Dencher, P. R., & Lake, M. (1996). A study of love-wave acoustic sensors. *Sensors and Actuators A: Physical*, 56(3), 211–219. [https://doi.org/10.1016/s0924-4247\(96\)01311-8](https://doi.org/10.1016/s0924-4247(96)01311-8)

Fan, X., White, I. M., Shopova, S. I., Zhu, H., Suter, J. D., & Sun, Y. (2008). Sensitive optical biosensors for unlabeled targets: A review. *Analytica Chimica Acta*, 620(1-2), 8–26. <https://doi.org/10.1016/j.aca.2008.05.022>

Fogel, R., Limson, J., & Seshia, A. A. (2016). Acoustic biosensors. *Essays in biochemistry*, 60(1), 101–110. <https://doi.org/10.1042/EBC20150011>

Gizeli, E., Bender, F., Rasmusson, A., Saha, K., Josse, F., & Cernosek, R. (2003). Sensitivity of the acoustic waveguide biosensor to protein binding as a function of the waveguide properties. *Biosensors and Bioelectronics*, 18(11), 1399–1406. [https://doi.org/10.1016/s0956-5663\(03\)00080-0](https://doi.org/10.1016/s0956-5663(03)00080-0)

Gizeli, E., Goddard, N. J., Lowe, C. R., & Stevenson, A. C. (1992). A Love plate biosensor utilising a polymer layer. *Sensors and Actuators B: Chemical*, 6(1-3), 131–137. [https://doi.org/10.1016/0925-4005\(92\)80044-x](https://doi.org/10.1016/0925-4005(92)80044-x)

Grammoustianou, A., & Gizeli, E. (2018). Acoustic Wave–Based Immunoassays. *Handbook of Immunoassay Technologies*, 203–239. <https://doi.org/10.1016/b978-0-12-811762-0.00009-8>

Greco, G., Agostini, M., Tonazzini, I., Sallemi, D., Barone, S., & Cecchini, M. (2018). Surface-Acoustic-Wave (SAW)-Driven Device for Dynamic Cell Cultures. *Analytical Chemistry*, 90(12), 7450–7457. <https://doi.org/10.1021/acs.analchem.8b00972>

Gronewold, T. M. A. (2007). Surface acoustic wave sensors in the bioanalytical field: Recent trends and challenges. *Analytica Chimica Acta*, 603(2), 119–128. <https://doi.org/10.1016/j.aca.2007.09.056>

Gubala, V., Harris, L. F., Ricco, A. J., Tan, M. X., & Williams, D. E. (2011). Point of care diagnostics: Status and future. *Analytical Chemistry*, 84(2), 487–515. <https://doi.org/10.1021/ac2030199>

- Haleem, A., Javid, M., Singh, R. P., Suman, R., & Rab, S. (2021). Biosensors applications in medical field: A brief review. *Sensors International*, 2, 100100. <https://doi.org/10.1016/j.sintl.2021.100100>
- Hales, M. C., & Burgess, J. W. (1976). Wide band monolithic crystal filters using lithium tantalate. *ElectroComponent Science and Technology*, 3(1), 43–49. <https://doi.org/10.1155/apec.3.43>
- Hamidon, M. N., & Yunusa, Z. (2016). Sensing materials for surface acoustic wave chemical sensors. *Progresses in Chemical Sensor*. <https://doi.org/10.5772/63287>
- Heineman, W. R., & Jensen, W. B. (2006). Leland C. Clark Jr. (1918–2005). *Biosensors and Bioelectronics*, 21(8), 1403–1404. <https://doi.org/10.1016/j.bios.2005.12.005>
- Huang, L., Ding, L., Zhou, J., Chen, S., Chen, F., Zhao, C., Xu, J., Hu, W., Ji, J., Xu, H., & Liu, G. L. (2021). One-step rapid quantification of SARS-COV-2 virus particles via low-cost nanoplasmonic sensors in generic microplate reader and point-of-care device. *Biosensors and Bioelectronics*, 171, 112685. <https://doi.org/10.1016/j.bios.2020.112685>
- Hughes, W. S. (1922). The potential difference between glass and electrolytes in contact with the glass. *Journal of the American Chemical Society*, 44(12), 2860–2867. <https://doi.org/10.1021/ja01433a021>
- Jakoby, B., & Vellekoop, M. J. (1997). Properties of love waves: Applications in sensors. *Smart Materials and Structures*, 6(6), 668–679. <https://doi.org/10.1088/0964-1726/6/6/003>
- Jo, M. C., & Guldiken, R. (2014). Effects of polydimethylsiloxane (PDMS) microchannels on surface acoustic wave-based microfluidic devices. *Microelectronic Engineering*, 113, 98–104. <https://doi.org/10.1016/j.mee.2013.07.021>
- Kaatze, U., & Uhlendorf, V. (1981). The dielectric properties of water at microwave frequencies. *Zeitschrift Für Physikalische Chemie*, 126(2), 151–165. <https://doi.org/10.1524/zpch.1981.126.2.151>
- Karunakaran, C., Rajkumar, R., & Bhargava, K. (2015). Introduction to Biosensors. *Biosensors and Bioelectronics*, 1–68. <https://doi.org/10.1016/b978-0-12-803100-1.00001-3>
- Kasper, M., Traxler, L., Salopek, J., Grabmayr, H., Ebner, A., & Kienberger, F. (2016). Broadband 120 MHz Impedance Quartz Crystal Microbalance (QCM) with Calibrated Resistance and Quantitative Dissipation for Biosensing Measurements at Higher Harmonic Frequencies. *Biosensors*, 6(2), 23. MDPI AG. <http://dx.doi.org/10.3390/bios6020023>
- Kucherenko, I., Soldatkin, A., Kucherenko, D., Soldatkina, O., & Dzyadevych, S. V. (2019). Advances in nanomaterial application in enzyme-based electrochemical biosensors: a review. *Nanoscale Advances*. <https://doi.org/10.1039/c9na00491b>

- Kumar, S., Nehra, M., Khurana, S., Dilbaghi, N., Kumar, V., Kaushik, A., & Kim, K.H. (2021). Aspects of point-of-care diagnostics for personalized health wellness. *International Journal of Nanomedicine*, 16, 383–402. <https://doi.org/10.2147/ijn.s267212>
- Kus, F., Altinkok, C., Zayim, E., Erdemir, S., Tasaltin, C., & Gurol, I. (2021). Surface acoustic wave (SAW) sensor for volatile organic compounds (VOCs) detection with calix[4]arene functionalized Gold nanorods (AuNRs) and silver nanocubes (AgNCs). *Sensors and Actuators B: Chemical*, 330, 129402. <https://doi.org/10.1016/j.snb.2020.129402>
- Lama, S., Kim, J., Ramesh, S., Lee, Y.-J., Kim, J., & Kim, J.-H. (2021). Highly Sensitive Hybrid Nanostructures for Dimethyl Methyl Phosphonate Detection. *Micromachines*, 12(6), 648. <https://doi.org/10.3390/mi12060648>
- Länge, K. (2019). Bulk and Surface Acoustic Wave Sensor Arrays for Multi-Analyte Detection: A Review. *Sensors*, 19(24), 5382. MDPI AG. <http://dx.doi.org/10.3390/s19245382>
- Länge, K., Rapp, B. E., & Rapp, M. (2008). Surface acoustic wave biosensors: A Review. *Analytical and Bioanalytical Chemistry*, 391(5), 1509–1519. <https://doi.org/10.1007/s00216-008-1911-5>
- Laude, V. (2021). Principles and properties of Phononic Crystal Waveguides. *APL Materials*, 9(8), 080701. <https://doi.org/10.1063/5.0059035>
- Lee, H., Hong, Y. J., Baik, S., Hyeon, T., & Kim, D.-H. (2018). Enzyme-Based Glucose Sensor: From Invasive to Wearable Device. *Advanced Healthcare Materials*, 7(8), 1701150. <https://doi.org/10.1002/adhm.201701150>
- Lei, Y., & Hu, H. (2020). SAW-driven droplet jetting technology in microfluidic: A review. *Biomicrofluidics*, 14(6), 061505. <https://doi.org/10.1063/5.0014768>
- Li, S., Sankaranarayanan, S. K., Fan, C., Su, Y., & Bhethanabotla, V. R. (2017). Achieving lower insertion loss and higher sensitivity in a saw biosensor via optimization of waveguide and microcavity structures. *IEEE Sensors Journal*, 17(6), 1608–1616. <https://doi.org/10.1109/jsen.2017.2651102>
- Majors, C. E., Smith, C. A., Natoli, M. E., Kundrod, K. A., & Richards-Kortum, R. (2017). Point-of-care diagnostics to improve maternal and neonatal health in low-resource settings. *Lab on a Chip*, 17(20), 3351–3387. <https://doi.org/10.1039/c7lc00374a>
- Malhotra, B. D., & Ali, M. A. (2018). Nanomaterials in Biosensors. *Nanomaterials for Biosensors*, 1–74. <https://doi.org/10.1016/b978-0-323-44923-6.00001-7>
- Malocha, D. C. (2004). Evolution of the saw transducer for communication systems. *IEEE Ultrasonics Symposium*, <https://doi.org/10.1109/ultsym.2004.1417726>

Mandal, D., & Banerjee, S. (2022). Surface Acoustic Wave (SAW) Sensors: Physics, Materials, and Applications. *Sensors*, 22(3), 820. MDPI AG. <http://dx.doi.org/10.3390/s22030820>

Mandal, D., & Banerjee, S. (2022). Surface Acoustic Wave (SAW) Sensors: Physics, Materials, and Applications. *Sensors*, 22(3), 820. MDPI AG. <http://dx.doi.org/10.3390/s22030820>

Mason, W. P. (1981). Piezoelectricity, its history and applications. *The Journal of the Acoustical Society of America*, 70(6), 1561–1566. <https://doi.org/10.1121/1.387221>

Mehrotra, P. (2016). Biosensors and their applications – A review. *Journal of Oral Biology and Craniofacial Research*, 6(2), 153–159. <https://doi.org/10.1016/j.jobcr.2015.12.002>

Mei, J., & Friend, J. (2019). A review: controlling the propagation of surface acoustic waves via waveguides for potential use in acoustofluidics. *Mechanical Engineering Reviews*. <https://doi.org/10.1299/mer.19-00402>

Mitsakakis, K., Tserepi, A., & Gizeli, E. (2008). Integration of microfluidics with a love wave sensor for the fabrication of a multisample analytical microdevice. *Journal of Microelectromechanical Systems*, 17(4), 1010–1019. <https://doi.org/10.1109/jmems.2008.927173>

Mitsakakis, K., Tsortos, A., Kondoh, J., & Gizeli, E. (2009). Parametric Study of SH-saw device response to various types of surface perturbations. *Sensors and Actuators B: Chemical*, 138(2), 408–416. <https://doi.org/10.1016/j.snb.2009.02.050>

Monošík, R., Stredánský, M., & Šturdík, E. (2012). Biosensors - classification, characterization and new trends. *Acta Chimica Slovaca*, 5(1) 109-120. <https://doi.org/10.2478/v10188-012-0017-z>

Moran, K. L. M., Lemass, D., & O’Kennedy, R. (2018). Surface Plasmon Resonance–Based Immunoassays. *Handbook of Immunoassay Technologies*, 129–156. <https://doi.org/10.1016/b978-0-12-811762-0.00006-2>

Morgan, D. P. (1998). History of saw devices. *Proceedings of the 1998 IEEE International Frequency Control Symposium* (Cat. No.98CH36165). <https://doi.org/10.1109/freq.1998.717937>

Na Songkhla, S., & Nakamoto, T. (2021). Overview of Quartz Crystal Microbalance Behavior Analysis and Measurement. *Chemosensors*, 9(12), 350. MDPI AG. <http://dx.doi.org/10.3390/chemosensors9120350>

Nair, M. P., Teo, A. J. T., & Li, K. H. H. (2021). Acoustic Biosensors and Microfluidic Devices in the Decennium: Principles and Applications. *Micromachines*, 13(1), 24. MDPI AG. <http://dx.doi.org/10.3390/mi13010024>

Naresh, V., & Lee, N. (2021). A Review on Biosensors and Recent Development of Nanostructured Materials-Enabled Biosensors. *Sensors*, 21(4), 1109. <https://doi.org/10.3390/s21041109>

Nguyen, H., Park, J., Kang, S., & Kim, M. (2015). Surface Plasmon Resonance: A Versatile Technique for Biosensor Applications. *Sensors*, 15(5), 10481–10510. MDPI AG. <http://dx.doi.org/10.3390/s150510481>

Nguyen, V. H., Peters, O., & Schnakenberg, U. (2017). One-port portable saw sensor system. *Measurement Science and Technology*, 29(1), 015107. <https://doi.org/10.1088/1361-6501/aa963f>

Notomi, T., Mori, Y., Tomita, N., & Kanda, H. (2015). Loop-mediated isothermal amplification (LAMP): principle, features, and future prospects. *Journal of Microbiology*, 53(1), 1–5. <https://doi.org/10.1007/s12275-015-4656-9>

Notomi, T., Okayama, H., Masubuchi, H., Yonekawa, T., Watanabe, K., Amino, N., & Hase, T. (2000). Loop-mediated isothermal amplification of DNA. *Nucleic acids research*, 28(12), E63. <https://doi.org/10.1093/nar/28.12.e63>

Odobashić, A., Šestan, I., & Begić, S. (2019). Biosensors for Determination of Heavy Metals in Waters. In T. Rincken, & K. Kivirand (Eds.), *Biosensors for Environmental Monitoring*. IntechOpen. <https://doi.org/10.5772/intechopen.84139>

Olson, N., & Bae, J. (2019). Biosensors-Publication Trends and Knowledge Domain Visualization. *Sensors (Basel, Switzerland)*, 19(11), 2615. <https://doi.org/10.3390/s19112615>

Panneerselvam, G., Thirumal, V., & Pandya, H.M. (2018). Review of Surface Acoustic Wave Sensors for the Detection and Identification of Toxic Environmental Gases/Vapours. *Archives of Acoustics*, 43, 357-367. <https://doi.org/10.24425/123908>.

Papadakis, G., Friedt, J. M., Eck, M., Rabus, D., Jobst, G., & Gizeli, E. (2017a). Optimized acoustic biochip integrated with microfluidics for biomarkers detection in molecular diagnostics. *Biomedical Microdevices*, 19(3). <https://doi.org/10.1007/s10544-017-0159-2>

Papadakis, G., Murasova, P., Hamiot, A., Tsougeni, K., Kaprou, G., Eck, M., Rabus, D., Bilkova, Z., Dupuy, B., Jobst, G., Tserepi, A., Gogolides, E., & Gizeli, E. (2018). Micro-nano-bio acoustic system for the detection of foodborne pathogens in real samples. *Biosensors and Bioelectronics*, 111, 52–58. <https://doi.org/10.1016/j.bios.2018.03.056>

Papadakis, G., Palladino, P., Chronaki, D., Tsortos, A., & Gizeli, E. (2017b). Sample-to-answer acoustic detection of DNA in complex samples. *Chemical Communications*, 53(57), 8058–8061. <https://doi.org/10.1039/c6cc10175e>

Peng, C. R., Liu, G., Zhong, H., & Shi, Y. (2021). Analysis of the influence of inductance and capacitance on film bulk acoustic wave filter. *IOP Conference Series: Materials Science and Engineering*, 1043(5), 052061. <https://doi.org/10.1088/1757-899x/1043/5/052061>

Peng, Y.-C., Cheng, C.-H., Yatsuda, H., Liu, S.-H., Liu, S.-J., Kogai, T., Kuo, C.-Y., et al. (2021). A Novel Rapid Test to Detect Anti-SARS-CoV-2 N Protein IgG Based on Shear Horizontal Surface Acoustic Wave (SH-SAW). *Diagnostics*, 11(10), 1838. MDPI AG. <http://dx.doi.org/10.3390/diagnostics11101838>

Peveler, W. J., Yazdani, M., & Rotello, V. M. (2016). Selectivity and Specificity: Pros and Cons in Sensing. *ACS Sensors*, 1(11), 1282–1285. <https://doi.org/10.1021/acssensors.6b00564>

Pitarke, J. M., Silkin, V. M., Chulkov, E. V., & Echenique, P. M. (2007). Theory of surface plasmons and surface-plasmon polaritons. *Reports on Progress in Physics*, 70(1), 1–87. <https://doi.org/10.1088/0034-4885/70/1/r01>

Pohanka, M. (2017). The Piezoelectric Biosensors: Principles and Applications, a Review. *International Journal of Electrochemical Science*, 496–506. <https://doi.org/10.20964/2017.01.44>

Polatoğlu, İ., Aydın, L., Nevruz, B. Ç., & Özer, S. (2020). A Novel Approach for the Optimal Design of a Biosensor. *Analytical Letters*, 1–18. <https://doi.org/10.1080/00032719.2019.1709075>

Prabowo, B. A., Purwidyantri, A., & Liu, K. C. (2018). Surface Plasmon Resonance Optical Sensor: A Review on Light Source Technology. *Biosensors*, 8(3), 80. <https://doi.org/10.3390/bios8030080>

Price, C. P. (2001). Regular review: Point of care testing. *BMJ*, 322(7297), 1285–1288. <https://doi.org/10.1136/bmj.322.7297.1285>

Prickril, B., & Rasooly, A. (Eds.). (2017). *Biosensors and Biodetection. Methods in Molecular Biology*. <https://doi.org/10.1007/978-1-4939-6911-1>

Primiceri, E., Chiriaco, M. S., Notarangelo, F. M., Crocamo, A., Ardissino, D., Cereda, M., Bramanti, A. P., Bianchessi, M. A., Giannelli, G., & Maruccio, G. (2018). Key Enabling Technologies for Point-of-Care Diagnostics. *Sensors (Basel, Switzerland)*, 18(11), 3607. <https://doi.org/10.3390/s18113607>

Priya, R., Thirumal, V., Pandiyarajan, G., & Pandya, H.M. (2014). SAW Devices – A Comprehensive Review. *Journal of Environmental Nanotechnology*. 3. 106-115. <https://doi.org/10.13074/jent.2014.09.143101>.

Priya, R., Thirumal, V., Pandiyarajan, G., & Pandya, H.M. (2015). A short review of SAW sensors. *Journal of Environmental Nanotechnology*. 4. <https://doi.org/10.13074/jent.2015.12.154171>.

- Rabus, D., Friedt, J., Ballandras, S., Martin, G., Carry, E., & Blondeau-Patissier, V. (2013). High-sensitivity open-loop electronics for gravimetric acoustic-wave-based sensors. *IEEE Transactions on Ultrasonics, Ferroelectrics, and Frequency Control*, 60(6), 1219–1226. <https://doi.org/10.1109/tuffc.2013.2685>
- Rabus, D., Martin, G., Carry, E., & Ballandras, S. (2012). Eight Channel Embedded Electronic Open Loop Interrogation for Multi Sensor Measurement. 2012 European Frequency and Time Forum. <https://doi.org/10.1109/efft.2012.6502420>
- Ramadan, K. S., Sameoto, D., & Evoy, S. (2014). A review of piezoelectric polymers as functional materials for electromechanical transducers. *Smart Materials and Structures*, 23(3), 033001. <https://doi.org/10.1088/0964-1726/23/3/033001>
- Rana, L., Gupta, R., Tomar, M., & Gupta, V. (2018). Highly sensitive love wave acoustic biosensor for uric acid. *Sensors and Actuators B: Chemical*, 261, 169–177. <https://doi.org/10.1016/j.snb.2018.01.122>
- Rasooly, A., & Herold, K. E. (Eds.). (2009). *Biosensors and Biodetection. Methods in Molecular Biology*. <https://doi.org/10.1007/978-1-60327-569-9>
- Rickert, J., Göpel, W., Hayward, G. L., Cavic, B. A., & Thompson, M. (1999). Biosensors Based on Acoustic Wave Devices. *Sensors Update*, 5(1), 105–139. [https://doi.org/10.1002/1616-8984\(199904\)5:1<105::aid-seup105>3.0.co;2-j](https://doi.org/10.1002/1616-8984(199904)5:1<105::aid-seup105>3.0.co;2-j)
- Rocha-Gaso, M.-I., March-Iborra, C., Montoya-Baides, Á., & Arnau-Vives, A. (2009). Surface generated acoustic wave biosensors for the detection of pathogens: A Review. *Sensors*, 9(7), 5740–5769. <https://doi.org/10.3390/s9095740>
- Ruppel, C. C. W. (2017). Acoustic Wave Filter Technology—A Review. *IEEE Transactions on Ultrasonics, Ferroelectrics, and Frequency Control*, 64(9), 1390–1400. <https://doi.org/10.1109/tuffc.2017.2690905>
- Rusling, J. F., & Forster, R. J. (2021). Biosensors Designed for Clinical Applications. *Biomedicines*, 9(7), 702. MDPI AG. <http://dx.doi.org/10.3390/biomedicines9070702>
- Saha, K., Bender, F., Rasmusson, A., & Gizeli, E. (2003). Probing the viscoelasticity and mass of a surface-bound protein layer with an acoustic waveguide device. *Langmuir*, 19(4), 1304–1311. <https://doi.org/10.1021/la026806p>
- Sajid, M., Kawde, A.-N., & Daud, M. (2015). Designs, formats and applications of lateral flow assay: A literature review. *Journal of Saudi Chemical Society*, 19(6), 689–705. <https://doi.org/10.1016/j.jscs.2014.09.001>
- Samarentsis, A. G., Pantazis, A. K., Tsortos, A., Friedt, J.-M., & Gizeli, E. (2020). Hybrid sensor device for simultaneous surface plasmon resonance and surface acoustic wave measurements. *Sensors*, 20(21), 6177. <https://doi.org/10.3390/s20216177>

- Sauerbrey, G. (1959). Use of oscillating crystals for weighing thin layers and for micro-weighing. *Journal of Physics*, 155(2), 206–222. <https://doi.org/10.1007/bf01337937>
- Sharma, A., Mishra, R. K., Goud, K. Y., Mohamed, M. A., Kummari, S., Tiwari, S., Li, Z., et al. (2021). Optical Biosensors for Diagnostics of Infectious Viral Disease: A Recent Update. *Diagnostics*, 11(11), 2083. MDPI AG. <http://dx.doi.org/10.3390/diagnostics11112083>
- Shiokawa, S., & Kondoh, J. (2004). Surface acoustic wave sensors. *Japanese Journal of Applied Physics*, 43(5B), 2799–2802. <https://doi.org/10.1143/jjap.43.2799>
- Shiokawa, S., & Moriizumi, T. (1988). Design of saw sensor in Liquid. *Japanese Journal of Applied Physics*, 27(S1), 142. <https://doi.org/10.7567/jjaps.27s1.142>
- Sirichaisinthop, J., Buates, S., Watanabe, R., Han, E. T., Suktawonjaroenpon, W., Krasaesub, S., Takeo, S., Tsuboi, T., & Sattabongkot, J. (2011). Evaluation of loop-mediated isothermal amplification (LAMP) for malaria diagnosis in a field setting. *The American journal of tropical medicine and hygiene*, 85(4), 594–596. <https://doi.org/10.4269/ajtmh.2011.10-0676>
- Sörensen, S.P.L. (1909) Über die messung und die bedeutung der wasserstoffionenkonzentration bei enzymatischen prozessen. *Enzymstudien. II. Mitteilung.* [On the measurement and the importance of hydrogen ion concentration during enzymatic processes. *Enzyme studies. 2nd Report.*]. *Biochem. Z.*, 21, 131–304.
- Stoukatch, S., Francis, L. A., Dupont, F., & Kraft, M. (2021). Low-cost microfluidic device micromachining and sequential integration with saw sensor intended for biomedical applications. *Sensors and Actuators A: Physical*, 319, 112526. <https://doi.org/10.1016/j.sna.2020.112526>
- Stradiotto, N. R., Yamanaka, H., & Zanoni, M. V. B. (2003). Electrochemical sensors: a powerful tool in analytical chemistry. *Journal of the Brazilian Chemical Society*, 14(2), 159–173. <https://doi.org/10.1590/s0103-50532003000200003>
- Syedmoradi, L., Norton, M. L., & Omidfar, K. (2021). Point-of-care cancer diagnostic devices: From academic research to clinical translation. *Talanta*, 225, 122002. <https://doi.org/10.1016/j.talanta.2020.122002>
- Tabbakh, T., Alotaibi, N., Almusaylim, Z. A., Alabdulkarim, S., Jhanjhi, N., & Darwish, N. B. (2021). Optoelectronics and Optical Bio-Sensors. In (Ed.), *Optoelectronics*. IntechOpen. <https://doi.org/10.5772/intechopen.96183>
- Tetyana, P., Shumbula, P. M., & Njengele-Tetyana, Z. (2021). Biosensors: Design, Development and Applications. In S. Ameen, M. S. Akhtar, & H. Shin (Eds.), *Nanopores*. IntechOpen. <https://doi.org/10.5772/intechopen.97576>

Tian, Y., Li, H., Chen, W., Lu, Z., Luo, W., Mu, X., & Wang, L. (2021). A Novel Love Wave Mode Sensor Waveguide Layer with Microphononic Crystals. *Applied Sciences*, 11(17), 8123. MDPI AG. <http://dx.doi.org/10.3390/app11178123>

Trivedi, S., & Nemade, H. B. (2017). Highly sensitive sh-saw resonator with SiO₂ trenches for biosensing application. *Materials Today: Proceedings*, 4(9), 10427–10431. <https://doi.org/10.1016/j.matpr.2017.06.393>

Tsortos, A., Papadakis, G., Mitsakakis, K., Melzak, K. A., & Gizeli, E. (2008). Quantitative determination of size and shape of surface-bound DNA using an acoustic wave sensor. *Biophysical Journal*, 94(7), 2706–2715. <https://doi.org/10.1529/biophysj.107.119271>

Voiculescu, I., & Nordin, A. N. (2012). Acoustic wave based MEMS devices for biosensing applications. *Biosensors and Bioelectronics*, 33(1), 1–9. <https://doi.org/10.1016/j.bios.2011.12.041>

Voinova, M. V. (2009). On Mass Loading and Dissipation Measured with Acoustic Wave Sensors: A Review. *Journal of Sensors*, 2009, 1–13. <https://doi.org/10.1155/2009/943125>

Wachiralurpan, S., Phung-On, I., Chanlek, N., Areekit, S., Chansiri, K., & Lieberzeit, P. A. (2021). In-Situ Monitoring of Real-Time Loop-Mediated Isothermal Amplification with QCM: Detecting *Listeria monocytogenes*. *Biosensors*, 11(9), 308. <https://doi.org/10.3390/bios11090308>

Wang, C., Liu, M., Wang, Z., Li, S., Deng, Y., & He, N. (2021). Point-of-care diagnostics for infectious diseases: From methods to devices. *Nano Today*, 37, 101092. <https://doi.org/10.1016/j.nantod.2021.101092>

Wang, S., Zhang, L., Xie, L., Huang, B., Zhang, A., Du, J., Wu, R., Wang, J., & Yong, Y.-K. (2018). Novel Quartz Crystal cuts for saw substrates with cubic frequency-temperature relations. 2018 IEEE International Ultrasonics Symposium (IUS). <https://doi.org/10.1109/ultsym.2018.8579853>

Wang, Y., Xu, H., Zhang, J., & Li, G. (2008). Electrochemical Sensors for Clinic Analysis. *Sensors*, 8(4), 2043–2081. MDPI AG. <http://dx.doi.org/10.3390/s8042043>

Warner, A. W., Onoe, M., & Coquin, G. A. (1967). Determination of elastic and piezoelectric constants for crystals in class (3M). *The Journal of the Acoustical Society of America*, 42(6), 1223–1231. <https://doi.org/10.1121/1.1910709>

White, R. M., & Voltmer, F. W. (1965). Direct piezoelectric coupling to surface elastic waves. *Applied Physics Letters*, 7(12), 314–316. <https://doi.org/10.1063/1.1754276>

Wohltjen, H., & Dessy, R. (1979). Surface acoustic wave probe for chemical analysis. I. introduction and instrument description. *Analytical Chemistry*, 51(9), 1458–1464. <https://doi.org/10.1021/ac50045a024>

Yager, P., Domingo, G. J., & Gerdes, J. (2008). Point-of-care diagnostics for global health. *Annual Review of Biomedical Engineering*, 10(1), 107–144. <https://doi.org/10.1146/annurev.bioeng.10.061807.160524>

Yandrapalli, S., Liffredo, M., Faizan, M., Kucuk, S., Maillard, D., & Villanueva, L. G. (2021). Thin Film Devices for 5G communications. 2021 IEEE 34th International Conference on Micro Electro Mechanical Systems (MEMS). <https://doi.org/10.1109/mems51782.2021.9375400>

Yoon, J., Shin, M., Lee, T., & Choi, J. W. (2020). Highly Sensitive Biosensors Based on Biomolecules and Functional Nanomaterials Depending on the Types of Nanomaterials: A Perspective Review. *Materials* (Basel, Switzerland), 13(2), 299. <https://doi.org/10.3390/ma13020299>

Zakaria, M.R., Farhi Shamsuddin, M.A., Hashim, U., Adam, T., & Al-Mufti, A.W. (2014). Design and Fabrication of IDT Surface Acoustic Wave Device for Biosensor Application. 2014 5th International Conference on Intelligent Systems, Modelling and Simulation, 760-764. <https://doi.org/10.1109/ISMS.2014.139>

Zanchetta, G., Lanfranco, R., Giavazzi, F., Bellini, T. & Buscaglia, M. (2017). Emerging applications of label-free optical biosensors. *Nanophotonics*, 6(4), 627-645. <https://doi.org/10.1515/nanoph-2016-0158>

Zhang, J., Wu, Q., Zhang, X., Wan, H., & Wang, P. (2021). Acoustic transducer and its applications in Biosensors. *Handbook of Cell Biosensors*, 517-535. https://doi.org/10.1007/978-3-030-23217-7_65

Zhang, J., Zhang, X., Wei, X., Xue, Y., Wan, H., & Wang, P. (2021). Recent advances in acoustic wave biosensors for the detection of disease-related biomarkers: A review. *Analytica Chimica Acta*, 1164, 338321. <https://doi.org/10.1016/j.aca.2021.338321>

Zhang, Y., Devendran, C., Lupton, C., de Marco, A., & Neild, A. (2018). Versatile platform for performing protocols on a chip utilizing surface acoustic wave (SAW) driven mixing. *Lab on a Chip*. <https://doi.org/10.1039/c8lc01117f>

Zida, S. I., Lin, Y., & Khung, Y. L. (2021). Current Trends on Surface Acoustic Wave Biosensors. *Advanced Materials Technologies*, 6(6), 2001018. <https://doi.org/10.1002/admt.202001018>

Appendices

The NanoVNASaver v0.3.9 software that was used for the purposes of the present dissertation can be downloaded from the following link: <https://github.com/NanoVNA-Saver/nanovna-saver/releases/tag/v0.3.9-pre>

The modified version of the software that was developed for real-time amplitude and phase measurements during the experiments of the present study can be downloaded from: <https://drive.google.com/drive/folders/1s10KIHYigvc5H0ormUb9YhAorxmO7vNL?usp=sharing>